Unfolded GARCH models

Xiaochun Liu[a], Richard Luger[b,*]

[a]*Department of Economics, Finance, and Insurance & Risk Management, University of Central Arkansas, Conway, AR 72035, USA*

[b]*Department of Finance, Insurance and Real Estate, Laval University, Quebec City, Quebec G1V 0A6, Canada*

June 2, 2015

ABSTRACT

A new GARCH-type model for autoregressive conditional volatility, skewness, and kurtosis is proposed. The approach decomposes returns into their signs and absolute values, and specifies the joint distribution by combining a multiplicative error model for the absolute values, a dynamic binary choice model for the signs, and a copula function for their interaction. The conditional volatility and kurtosis are determined by innovations following a folded (or absolute) Student-t distribution with time-varying degrees of freedom, and separate time variation in conditional return skewness is achieved by allowing the copula parameter to be dynamic. Model estimation is performed with Bayesian methods using an adaptive Markov chain Monte Carlo algorithm. An empirical application to the returns on four major international stock market indices illustrates the statistical and economic significance of the new model for conditional higher moments.

JEL classification: C11, C22, C58

Keywords: Conditional skewness and kurtosis; Direction-of-change model; Absolute returns; Folded distribution; Copula model; Adaptive MCMC.

*Corresponding author. Tel.: +1 418 656 2131 ext. 6229.

E-mail addresses: xliu@uca.edu (X. Liu), richard.luger@fsa.ulaval.ca (R. Luger).

1 Introduction

Consider a daily financial return at time t, denoted by R_t, which is assumed to be continuously distributed. It is quite common in empirical studies to see models of the form:

$$R_t = \sigma_t \varepsilon_t, \tag{1}$$

where the conditional variance σ_t^2 is specified as a generalized autoregressive conditional heteroskedasticity (GARCH) model. In GARCH models *à la* Bollerslev (1987), the innovation ε_t in (1) is assumed to be distributed according to a symmetric Student-t distribution with ν degrees of freedom. Such a model implies that the conditional distribution of R_t has a time-varying variance, but a mean and skewness of zero, and constant kurtosis. Recognizing that returns may in fact be better characterized by a conditional distribution with time-varying asymmetry and tail heaviness can have important implications for many problems in finance, e.g. for asset allocation, value-at-risk calculations, or the valuation of contingent claims.

Several studies consider the modeling of conditional moments beyond order two. For instance, Harvey and Siddique (1999) propose a model based on a non-central Student-t distribution that allows for time-varying conditional variance and skewness. They apply their model to the daily returns on several stock market indices and find that autoregressive conditional skewness plays an important role in return dynamics. This approach allows for time variation in the conditional skewness, but it still assumes a constant kurtosis. Brooks et al. (2005) (BBHP) develop a model for autoregressive conditional kurtosis by allowing the degrees-of-freedom parameter of a central Student-t distribution to vary over time. The resulting model permits the kurtosis to vary separately from the variance, but cannot produce asymmetric returns. So while Harvey and Siddique focus on the third moment at the expense of the fourth, the BBHP approach focuses on the fourth moment at the expense of the third. Brooks et al. (2005) argue that it is more important to allow for time variation in the conditional kurtosis.

Jondeau and Rockinger (2003) propose an approach for the joint modeling of conditional skewness and kurtosis. Their starting point is the generalized Student-t distribution proposed by Hansen (1994) which introduces an additional parameter that imparts asymmetry. Jondeau and Rockinger propose specifications for the dynamics of the degrees-of-freedom and asymmetry parameters, and show how these values map into the usual coefficients of skewness and kurtosis. This approach is very restrictive as the dynamics of skewness and kurtosis cannot be disentangled from each other. Indeed, variation in the asymmetry parameter necessarily entails changes in both the third and fourth moments. As Jondeau and Rockinger (2003) explain, the tight link between skewness and kurtosis, in addition to restrictions on the underlying parameters, makes estimation of this model very difficult; see also the discussion in Jondeau et al. (2007, §5.5) for more on this point. León et al. (2005) (LRS) propose a completely different GARCH-type model that circumvents the problems of the Jondeau-Rockinger approach. The LRS model is based on a Gram-Charlier series expansion of an assumed normal density function for the innovation terms in (1), truncated at the fourth moment. The result is a more flexible specification in the sense that it allows for time variation in skewness and/or kurtosis, in addition to autoregressive conditional variances. The empirical results presented by LRS suggest the presence of conditional skewness and kurtosis in daily stock index returns. The potential shortcoming of the LRS approach, however, is that it requires the truncation of the Gram-Charlier expansion and may thus provide a poor approximation to the true return distribution (Del Brio and Perote, 2012).

In this paper, we propose a new and very flexible approach to modeling conditional higher moments. Following Anatolyev and Gospodinov (2010), our approach starts by decomposing returns into their signs and absolute values. The joint distribution of return signs and absolute values is then obtained by combining a multiplicative error model for the absolute returns, a dynamic binary choice model for the signs, and a copula joining function for their interaction. Here the innovations follow a folded (or absolute) Student-t distribution with time-varying degrees of freedom, which allows for autoregressive conditional return kurtosis. Separate time variation in conditional return skewness is achieved by allowing the copula parameter to have its own autoregressive dynamics. The equations governing the dynamics of second, third, and fourth conditional moments are very similar to those of the usual GARCH framework. We refer to the resulting models as "unfolded" GARCH models, as the approach takes a folded distribution for the absolute returns and transforms it into a distribution for the returns themselves by joining their signs with the absolute values. The BBHP model is a special case of this approach that obtains under the independence copula specification, which in turn nests the Bollerslev (1987) specification with constant conditional kurtosis. Another interesting feature of the proposed copula model is that the conditional expectation of returns need not be zero, since its (possibly time-varying) value depends on the interaction between signs and absolute return values.

The rest of the paper is organized as follows. Section 2 describes the proposed methodology by first presenting the models for the marginal distributions of signs and absolute return values, and the copula model for their interaction. The likelihood function is then derived, followed by a discussion of how to compute the model-implied conditional mean, variance, skewness, and kurtosis. Section 3 presents our Bayesian estimation method based on the adaptive Markov chain Monte Carlo (MCMC) scheme of Gerlach et al. (2011) and Chen et al. (2012). Section 4 begins by presenting some simulation results about the performance of the MCMC sampler for posterior inference with the proposed model. This section then moves on to an empirical analysis of the daily returns on four major international stock market indices. For comparison purposes, we consider several other models that are close to our proposed specification, including the BBHP and LRS models. We evaluate the relative performance of the competing models using both in-sample and out-of-sample statistical comparisons. In addition, we provide evidence regarding the economic significance of these models in the context of a risk management application. Section 5 concludes.

2 Model description

Consider again the daily financial return R_t in (1), but now observe that it can be decomposed as

$$\begin{aligned} R_t &= |R_t| \operatorname{sign}(R_t) \\ &= |R_t| (2S_t - 1), \end{aligned} \tag{2}$$

where $S_t = \mathbb{I}[R_t > 0]$ and $\mathbb{I}[A]$ is the indicator function of event A. Our model specifies marginal distributions for $|R_t|$ and S_t, and a copula for the interaction of these two random variables. Observe also that with this approach the mean of R_t need not be exactly zero every day. Indeed, the decomposition in (2) implies that $\mu_t = E(R_t \,|\, \mathfrak{F}_{t-1})$ is given by

$$\mu_t = 2\xi_t - E(|R_t| \,|\, \mathfrak{F}_{t-1}), \tag{3}$$

where $\xi_t = E(|R_t| S_t \,|\, \mathfrak{F}_{t-1})$ is the expected cross-product of $|R_t|$ and S_t, and the expectations are conditional on $\mathfrak{F}_{t-1}$, the information set available at time $t-1$. The conditional distribution of S_t is of course Bernoulli $\mathcal{B}(p_t \,|\, \mathfrak{F}_{t-1})$, where p_t denotes the conditional probability $\Pr(R_t > 0 \,|\, \mathfrak{F}_{t-1}) = E(S_t \,|\, \mathfrak{F}_{t-1})$. The next subsections describe the models for p_t and $|R_t|$, and the copula model specifications. Observe first that if R_t is symmetrically distributed around zero, then $|R_t|$ and S_t are independent and $p_t = 1/2$ (Randles and Wolfe, 1979, Lemma 2.4.2). In this case, $E(S_t \,|\, \mathfrak{F}_{t-1}) = 1/2$ and hence $\mu_t = 0$. If on the contrary $|R_t|$ and S_t are not independent, then the distribution of R_t is asymmetric and μ_t may change over time depending on how $|R_t|$ and S_t interact. Since μ_t is free in this context, we proceed by specifying the uncentered moments of R_t and then show how to find the model-implied centered moments.

2.1 Marginal distributions

The absolute value of the return appearing in (2) is modeled in multiplicative form as

$$|R_t| = \lambda_t \, |\varepsilon_t|, \tag{4}$$

where λ_t is $\mathfrak{F}_{t-1}$-measurable and $|\varepsilon_t|$ follows an absolute distribution, also called a *folded* distribution by Leone et al. (1961) and Psarakis and Panaretos (1990) who introduce the folded normal and Student-t distributions, respectively. To better understand these so-called "folded" distributions, suppose there exists an underlying random variable ε_t whose conditional distribution given $\mathfrak{F}_{t-1}$ is continuous and symmetric around zero. Let $g_{\varepsilon_t}(x \,|\, \mathfrak{F}_{t-1})$ and $G_{\varepsilon_t}(x \,|\, \mathfrak{F}_{t-1})$ denote the conditional density and distribution functions, respectively, of ε_t. Folding $g_{\varepsilon_t}(x \,|\, \mathfrak{F}_{t-1})$ at $x = 0$ results in the distribution of the random variable $|\varepsilon_t|$ whose conditional distribution function is defined as

$$F_{|\varepsilon_t|}(x \,|\, \mathfrak{F}_{t-1}) = 2G_{\varepsilon_t}(x \,|\, \mathfrak{F}_{t-1}) - 1, \text{ for } x \geq 0, \tag{5}$$

which, upon differentiation, is equivalent to $f_{|\varepsilon_t|}(x \,|\, \mathfrak{F}_{t-1}) = 2g_{\varepsilon_t}(x \,|\, \mathfrak{F}_{t-1})$, $x \geq 0$, in terms of the conditional probability density functions. It is also easy to see that the even moments of $|\varepsilon_t|$ and ε_t are identical.

We assume that the random term $|\varepsilon_t|$ in (4) is independent and identically distributed (i.i.d.) as a folded Student-t variate with degrees-of-freedom parameter ν_t, conditional on $\mathfrak{F}_{t-1}$. The conditional second and fourth moments of (4) are then given by

$$m_{2,R_t} = \lambda_t^2 \frac{\nu_t}{(\nu_t - 2)}, \tag{6}$$

$$m_{4,R_t} = \lambda_t^4 \frac{3\nu_t^2}{(\nu_t - 2)(\nu_t - 4)}, \tag{7}$$

respectively. Rearranging (6) shows that λ_t can be expressed as

$$\lambda_t = \left(m_{2,R_t} \frac{(\nu_t - 2)}{\nu_t} \right)^{1/2}, \tag{8}$$

which, upon substitution in (7), can then be used to find that

$$\nu_t = \frac{2(2m_{4,\varepsilon_t^*} - 3)}{m_{4,\varepsilon_t^*} - 3}, \tag{9}$$

where $|\varepsilon_t^*| = |\varepsilon_t|\sqrt{(\nu_t - 2)/\nu_t}$ is the innovation term in (4) standardized to have a second moment equal to unity. These last two equations show that the dynamics of ν_t and λ_t are determined by those of m_{2,R_t} and $m_{4,\varepsilon_t^*} = m_{4,R_t}/m_{2,R_t}^2$, which may be modeled separately with the restriction that $\nu_t > 4$ to ensure the existence of the fourth moment in (7) and hence that of the second moment in (6). Observe that these requirements also guarantee that $\lambda_t > 0$ in (4).

Similarly to Brooks et al. (2005) who model time-varying conditional variance and kurtosis, we parameterize the conditional second and fourth moments, m_{2,R_t} and m_{4,ε_t^*}, as GARCH-type processes, expressed as

$$\begin{aligned} m_{2,R_t} &= \omega_0 + \omega_1 R_{t-1}^2 + \omega_2 m_{2,R_{t-1}}, \\ m_{4,\varepsilon_t^*} &= \delta_0 + \delta_1 \frac{R_{t-1}^4}{m_{2,R_{t-1}}^2} + \delta_2 m_{4,\varepsilon_{t-1}^*}, \end{aligned}$$

with the following restrictions to ensure positivity and stationarity: $\omega_0, \delta_0 > 0$, $\omega_1, \omega_2, \delta_1, \delta_2 \geq 0$, and $\omega_1 + \omega_2 < 1$, $\delta_1 + \delta_2 < 1$. Observe from (9) that $\nu_t \to \infty$ implies that $m_{4,R_t}/m_{2,R_t}^2 \to 3$, the standardized fourth moment of the folded normal distribution. The parameters describing the marginal distribution of $|R_t|$ are grouped into $\boldsymbol{\theta}_1 = (\omega_0, \omega_1, \omega_2, \delta_0, \delta_1, \delta_2)$, with the additional restriction $4 < \nu_t < 30$ to ensure a proper posterior density (Bauwens and Lubrano, 1998).

As we already mentioned, the conditional distribution of S_t is Bernoulli $\mathcal{B}(p_t \,|\, \mathfrak{F}_{t-1})$ with probability mass function $f_{S_t}(v \,|\, \mathfrak{F}_{t-1}) = p_t^v(1-p_t)^{1-v}$, where $p_t = \Pr(R_t > 0 \,|\, \mathfrak{F}_{t-1})$. Following Anatolyev and Gospodinov (2010), we parametrize p_t as a dynamic logit model of the form

$$p_t = \frac{\exp(\theta_t)}{1 + \exp(\theta_t)} \tag{10}$$

with

$$\theta_t = \varphi_0 + \varphi_1 R_{t-1}^2 + \varphi_2 S_{t-1} + \varphi_3 \theta_{t-1},$$

which resembles a GARCH equation. The inclusion of R_{t-1}^2 on the right-hand side is motivated by the work of Christoffersen and Diebold (2006) who show that volatility dynamics can generate time variation in $\Pr(R_t > 0 \,|\, \mathfrak{F}_{t-1})$. It is interesting to note that the dynamic logit model can be rewritten as

$$\log \frac{p_t}{1 - p_t} = \varphi_0 + \varphi_1 R_{t-1}^2 + \varphi_2 S_{t-1} + \varphi_3 \log \frac{p_{t-1}}{1 - p_{t-1}},$$

making clear how the (log of the) odds that $R_t > 0$ at time t depend on their lagged values. We stack all the parameters into $\boldsymbol{\theta}_2 = (\varphi_0, \varphi_1, \varphi_2, \varphi_3)$ and impose $|\varphi_2|, |\varphi_3| < 1$ to ensure stationary dynamics. See de Jong and Woutersen (2011) for more on dynamic binary choice models.

2.2 Joint distribution

In order to construct the bivariate distribution of $Y_t = (|R_t|, S_t)'$, we appeal to the theory of copulas; see, e.g. Trivedi and Zimmer (2005) and Patton (2012) for recent surveys. Specifically, it is well known that a conditional meta-distribution can be created as

$$F_{Y_t}(u, v \,|\, \mathfrak{F}_{t-1}) = C\big(F_{|R_t|}(u \,|\, \mathfrak{F}_{t-1}), F_{S_t}(v \,|\, \mathfrak{F}_{t-1}) \,\big|\, \mathfrak{F}_{t-1}\big),$$

where $F_{|R_t|}(u \,|\, \mathfrak{F}_{t-1})$ and $F_{S_t}(v \,|\, \mathfrak{F}_{t-1})$ are the conditional distribution functions of $|R_t|$ and S_t, respectively, and $C(w_1, w_2 \,|\, \mathfrak{F}_{t-1})$ is a conditional copula distribution function with dependency parameter α_t. From Anatolyev and Gospodinov (2010), the joint conditional density/mass function of $|R_t|$ and S_t is given by

$$f_{Y_t}(u, v \,|\, \mathfrak{F}_{t-1}) = f_{|R_t|}(u \,|\, \mathfrak{F}_{t-1}) \varrho_t\big(F_{|R_t|}(u \,|\, \mathfrak{F}_{t-1})\big)^v \Big(1 - \varrho_t\big(F_{|R_t|}(u \,|\, \mathfrak{F}_{t-1})\big)\Big)^{1-v}, \tag{11}$$

where $\varrho_t(z) = 1 - \partial C(z, 1 - p_t \,|\, \mathfrak{F}_{t-1}) / \partial w_1$. Observe that (11) is a product of the marginal density of $|R_t|$ and the "deformed" Bernoulli mass of S_t whose success probability is given by $\varrho_t\big(F_{|R_t|}(u \,|\, \mathfrak{F}_{t-1})\big)$, which need not equal p_t.

The copula parameter measures the dependence between $|R_t|$ and S_t. Indeed, recall that if R_t is symmetric, then $|R_t|$ and S_t are independent. On the other hand, negative (positive) skewness means that the dependence between $|R_t|$ and S_t is negative (positive). To capture the potentially time-varying conditional return skewness, we parameterize the copula parameter as

$$\alpha_t = b_0 + b_1 |R_{t-1}|(1 - S_{t-1}) + b_2 \alpha_{t-1}, \tag{12}$$

which is an example of what Manner and Reznikova (2012) call an "observation driven" copula model. Here the forcing variable is $|R_{t-1}|(1 - S_{t-1})$, which equals $|R_{t-1}|$ when R_{t-1} is negative, and zero otherwise. This choice is motivated by the fact again that if daily returns are skewed, then we expect it to be mostly left skewness. The parameters of (12) are regrouped in $\boldsymbol{\theta}_3 = (b_0, b_1, b_2)$. Depending on the copula, additional restrictions may be needed to ensure that α_t is admissible. Below we list four choices of bivariate copulas that will be used in the empirical application. Since they are well known, we only give very brief descriptions.

Frank copula. The conditional Frank copula is

$$C(w_1, w_2 \,|\, \mathfrak{F}_{t-1}) = -\frac{1}{\alpha_t} \log\left(1 + \frac{(e^{-\alpha_t w_1} - 1)(e^{-\alpha_t w_2} - 1)}{e^{-\alpha_t} - 1}\right),$$

where $\alpha_t < 0$ ($\alpha_t > 0$) implies negative (positive) dependence. As $\alpha_t \to 0$, the Frank copula approaches the independence copula, $C(w_1, w_2) = w_1 w_2$. Therefore we define the function $\varrho_t(z)$ appearing in (11) as

$$\varrho_t(z) = \begin{cases} \left(1 - \frac{1-e^{-\alpha_t(1-p_t)}}{1-e^{\alpha_t p_t}} e^{\alpha_t(1-z)}\right)^{-1}, & \text{for } \alpha_t \neq 0, \\ p_t, & \text{for } \alpha_t = 0. \end{cases}$$

Farlie-Gumbel-Morgenstern copula. The conditional Farlie-Gumbel-Morgenstern (FGM) copula is

$$C(w_1, w_2 \,|\, \mathfrak{F}_{t-1}) = w_1 w_2 \big(1 + \alpha_t (1 - w_1)(1 - w_2)\big)$$

where $\alpha_t \in [-1, 1]$ and $\alpha_t < 0$ ($\alpha_t > 0$) implies negative (positive) dependence. Note that this copula only permits modest dependence, which is not restrictive in our application. The $\varrho_t(z)$ function appearing in (11) is given as

$$\varrho_t(z) = 1 - (1 - p_t)\big(1 + \alpha_t p_t (1 - 2z)\big),$$

with $\varrho_t(z) = p_t$ when $\alpha_t = 0$, i.e. when the marginals are independent. In order to ensure that $\alpha_t \in [-1, 1]$, we follow Almeida and Czado (2012) and reparametrize the FGM copula dynamics as

$$\alpha_t = \frac{\exp(2\phi_t) - 1}{\exp(2\phi_t) + 1},$$

with $\phi_t = b_0 + b_1 |R_{t-1}|(1 - S_{t-1}) + b_2 \phi_{t-1}$ instead of (12).

Rotated Clayton copulas. The conditional Clayton copula is given by

$$C(w_1, w_2 \,|\, \mathfrak{F}_{t-1}) = (w_1^{-\alpha_t} + w_2^{-\alpha_t} - 1)^{-1/\alpha_t},$$

where $\alpha_t > 0$. The Clayton copula tends to the independence copula as $\alpha_t \to 0$. The $\varrho_t(z)$ function appearing in (11) is thus given as

$$\varrho_t(z) = \begin{cases} 1 - \left(1 + \frac{(1-p_t)^{-\alpha_t}-1}{z^{-\alpha_t}}\right)^{-1/\alpha_t - 1}, & \text{for } \alpha_t > 0, \\ p_t, & \text{for } \alpha_t = 0. \end{cases}$$

The Clayton copula cannot account for negative dependence. Since we expect daily financial returns to exhibit negative skewness, if at all, we follow Patton (2012) and consider rotated Clayton copulas. A 90° rotation results by flipping the first variable so that $(1 - W_1, W_2)$ is distributed as a Clayton copula with parameter α_t. Large values of α_t then imply stronger negative dependence and tail dependence in the second quadrant (i.e. as $w_1 \to 1$ and $w_2 \to 0$) rather than the third quadrant as for the usual Clayton copula. A 270° rotation of the Clayton copula also implies negative dependence, but with tail dependence in the fourth quadrant (i.e. as $w_1 \to 0$ and $w_2 \to 1$). We use RC90 and RC270 to denote these rotated Clayton copulas and both are considered in our empirical application. Here we impose the restriction $\alpha_t > 0$ via the reparametrization $\alpha_t = \exp(\phi_t)$ with $\phi_t = b_0 + b_1|R_{t-1}|(1 - S_{t-1}) + b_2\phi_{t-1}$ instead of (12).

2.3 Special cases

We call the developed model for R_t an *unfolded* GARCH (UnGARCH) model as it "unfolds" $|R_t|$ into $R_t = |R_t|(2S_t - 1)$, where $|R_t| = \lambda_t|\varepsilon_t|$ with the scale and copula parameters (λ_t, α_t) determined by GARCH-type processes.

The UnGARCH model nests three other GARCH specifications. Indeed, if S_t is i.i.d. $\mathcal{B}(1/2)$, then the model innovations follow symmetric Student-t distributions and R_t is governed by the autoregressive conditional kurtosis model of Brooks et al. (2005) given here as

$$R_t = \lambda_t\varepsilon_t, \quad \varepsilon_t \,|\, \mathfrak{F}_{t-1} \sim t_{\nu_t}, \tag{13}$$

$$\lambda_t = \left(\sigma_t^2 \frac{(\nu_t - 2)}{\nu_t}\right)^{1/2} \tag{14}$$

$$\sigma_t^2 = \omega_0 + \omega_1 R_{t-1}^2 + \omega_2\sigma_{t-1}^2, \tag{15}$$

$$k_t = \delta_0 + \delta_1 \frac{R_{t-1}^4}{\sigma_{t-1}^4} + \delta_2 k_{t-1}, \tag{16}$$

$$\nu_t = \frac{2(2k_t - 3)}{k_t - 3}, \tag{17}$$

where t_{ν_t} denotes a Student-t distribution with ν_t degrees of freedom. The BBHP specification is a special case of the UnGARCH model which occurs when $|R_t|$ and S_t are joined by the independence copula ($\alpha_t = 0$) and when $\varphi_i = 0$, $i = 0, ..., 3$, so that $p_t = 1/2$ in (10). If furthermore ν_t in (17) is constant over time so that $\delta_1 = \delta_2 = 0$, then the model becomes a GARCH specification with i.i.d. innovations according to a symmetric Student-t distibution *à la* Bollerslev (1987). And when the degrees of freedom tend to infinity, the Student-t distribution collapses to the normal one.

In the empirical application presented in Section 4, we estimate the UnGARCH model allowing for a time-varying conditional return skewness and we formally compare it to the nested BBHP specification in (13)–(17) which imposes conditional return symmetry each time period.

2.4 Likelihood function

Assuming a folded Student-t distribution for $|\varepsilon_t|$ means that the conditional density of $|R_t|$ is given by

$$f_{|R_t|}(x \,|\, \mathfrak{F}_{t-1}) = \frac{2}{\lambda_t} \frac{\Gamma\left(\frac{\nu_t+1}{2}\right)}{\sqrt{\nu_t \pi}\,\Gamma\left(\frac{\nu_t}{2}\right)} \left(1 + \frac{x^2}{\lambda_t^2 \nu_t}\right)^{-\frac{\nu_t+1}{2}}, \text{ for } x \geq 0, \tag{18}$$

where the leading term $1/\lambda_t$ is the Jacobian factor which arises from (4) upon taking the derivative of $|\varepsilon_t|$ with respect to $|R_t|$. The corresponding conditional distribution function is simply $F_{|R_t|}(x \,|\, \mathfrak{F}_{t-1}) = F_{|\varepsilon_t|}(x/\lambda_t \,|\, \mathfrak{F}_{t-1})$, $x \geq 0$, where the latter distribution function is given by (5).

The complete set of model parameters is $\boldsymbol{\Theta} = (\boldsymbol{\theta}_1, \boldsymbol{\theta}_2, \boldsymbol{\theta}_3)$, comprising the parameters of: (i) the marginal distribution of $|R_t|$, (ii) the marginal distribution of S_t, and (iii) the copula distribution. Given a sample of returns $r_1, ..., r_T$, which yield the realizations $\boldsymbol{y} = \big((|r_1|, s_1), ..., (|r_T|, s_T)\big)$, the sample likelihood function can be computed from (11) as

$$L(\boldsymbol{y}|\boldsymbol{\Theta}) = \prod_{t=1}^{T} \varrho_t\big(F_{|R_t|}(|r_t| \,|\, \mathfrak{F}_{t-1})\big)^{s_t} \Big\{1 - \varrho_t\big(F_{|R_t|}(|r_t| \,|\, \mathfrak{F}_{t-1})\big)\Big\}^{1-s_t} f_{|R_t|}(|r_t| \,|\, \mathfrak{F}_{t-1}), \tag{19}$$

where $\boldsymbol{\Theta}$ belongs to $\boldsymbol{\Xi}$, a set of values satisfying the model's restrictions. With the Bayesian inference approach, we follow Geweke (1988, 1989) and impose any model restrictions that take the form of inequalities through the prior; i.e., we retain only the draws that satisfy the inequalities when sampling the posterior distribution.

2.5 Conditional mean, variance, skewness, and kurtosis

In this subsection, we explain how to compute the model-implied conditional mean, variance, skewness, and kurtosis of returns. Recall from (3) that in order to compute the conditional mean $\mu_t = E(R_t \,|\, \mathfrak{F}_{t-1})$, we need ξ_t and $E(|R_t| \,|\, \mathfrak{F}_{t-1})$. The latter term is found from (4) as $E(|R_t| \,|\, \mathfrak{F}_{t-1}) = \lambda_t E(|\varepsilon_t| \,|\, \mathfrak{F}_{t-1})$ with λ_t given by (8) and where

$$E(|\varepsilon_t| \,|\, \mathfrak{F}_{t-1}) = 2\sqrt{\frac{\upsilon_t}{\pi}} \frac{\Gamma\left(\frac{\upsilon_t+1}{2}\right)}{\Gamma\left(\frac{\upsilon_t}{2}\right)(\upsilon_t - 1)}$$

is found in Psarakis and Panaretos (1990). The term ξ_t is given by Anatolyev and Gospodinov (2010) as

$$\xi_t = \int_0^{+\infty} u f_{|R_t|}(u \,|\, \mathfrak{F}_{t-1}) \varrho_t\big(F_{|R_t|}(u \,|\, \mathfrak{F}_{t-1})\big) du,$$

which must be evaluated numerically. Upon the change of variable $z = F_{|R_t|}(u \,|\, \mathfrak{F}_{t-1})$, this integral can be rewritten as

$$\xi_t = \int_0^1 F^{-1}_{|R_t|}(z \,|\, \mathfrak{F}_{t-1}) \varrho_t(z) dz, \tag{20}$$

where $F^{-1}_{|R_t|}(z \,|\, \mathfrak{F}_{t-1})$ is the quantile function of $F_{|R_t|}(u \,|\, \mathfrak{F}_{t-1})$. From (5), we have that

$$F^{-1}_{|R_t|}(z \,|\, \mathfrak{F}_{t-1}) = \lambda_t \, G^{-1}_{\varepsilon_t}\left(\frac{z+1}{2} \,|\, \mathfrak{F}_{t-1}\right),$$

where G^{-1} is the quantile function of a Student-t distribution with ν_t degrees of freedom.

With μ_t in hand, the conditional variance of R_t is computed as

$$\mathrm{Var}(R_t \,|\, \mathfrak{F}_{t-1}) = m_{2,R_t} - \mu_t^2, \tag{21}$$

where m_{2,R_t} is given directly by (6). In turn, it is then straightforward to numerically evaluate the usual coefficients of conditional skewness and kurtosis via

$$\mathrm{Sk}(R_t \,|\, \mathfrak{F}_{t-1}) = E\left[\left(\frac{R_t - \mu_t}{\sigma_t}\right)^3 \,|\, \mathfrak{F}_{t-1}\right], \tag{22}$$

$$\mathrm{Ku}(R_t \,|\, \mathfrak{F}_{t-1}) = E\left[\left(\frac{R_t - \mu_t}{\sigma_t}\right)^4 \,|\, \mathfrak{F}_{t-1}\right], \tag{23}$$

where $\sigma_t = \sqrt{\mathrm{Var}(R_t \,|\, \mathfrak{F}_{t-1})}$ is the conditional standard deviation of R_t. In our empirical application, we evaluate (20), (22), and (23) by Monte Carlo integration once the parameter estimates are obtained.

3 Bayesian inference

The UnGARCH model is highly non-linear and also depends on the absolute value and indicator functions, which introduce kinks and discontinuities into the sample likelihood function in (19). This feature makes it very difficult to use classical methods for maximum likelihood estimation and inference, so we instead prefer to use Bayesian MCMC methods to learn about the model parameters. Given the sample realizations, $\boldsymbol{y}$, the posterior distribution takes the usual form: $p(\boldsymbol{\Theta}|\boldsymbol{y}) \propto L(\boldsymbol{y}|\boldsymbol{\Theta})\pi(\boldsymbol{\Theta})$, where $L(\boldsymbol{y}|\boldsymbol{\Theta})$ is the sample likelihood function and $\pi(\boldsymbol{\Theta})$ is the prior distribution. The prior distribution is taken as uniform over $\boldsymbol{\Xi}$, the admissible parameter space. Just like Vrontos et al. (2002) and Ausin and Lopes (2010), we also found that MCMC mixing can be improved and the computational cost reduced by using simultaneous updating of the highly correlated parameter groups at each Metropolis-Hastings (MH) step. In the terminology of Chib and Greenberg (1995), our approach is therefore based on a "block-at-a-time" MH sampler which updates successively the parameter blocks comprising $\boldsymbol{\Theta} = (\boldsymbol{\theta}_1, \boldsymbol{\theta}_2, \boldsymbol{\theta}_3)$.

We implement the MH sampler according to the adaptive scheme of Gerlach et al. (2011) and Chen et al. (2012) which combines the random walk MH and the independent kernel MH algorithms, each based on a mixture of multivariate normal distributions. The random walk part of this scheme is designed to allow occasional large jumps, perhaps away from local modes, thereby improving the chances that the Markov chain will explore the posterior distribution. Let $\boldsymbol{\Theta}_{-i}$ denote the vector $\boldsymbol{\Theta}$ excluding the block $\boldsymbol{\theta}_i$.

Starting at $k = 1$ with $\boldsymbol{\Theta}^{[1]} = (\boldsymbol{\theta}_1^{[1]}, \boldsymbol{\theta}_2^{[1]}, \boldsymbol{\theta}_3^{[1]})$, the K_1 random walk MH iterations for $\boldsymbol{\Theta}$ proceed as follows:

Step 1. Increment k by 1 and set $\boldsymbol{\Theta}^{[k]}$ equal to $\boldsymbol{\Theta}^{[k-1]}$.

Step 2. For $i = 1, 2, 3$ in turn, generate $\boldsymbol{\theta}_i^p$ as

$$\boldsymbol{\theta}_i^p = \boldsymbol{\theta}_i^{[k]} + \boldsymbol{\varepsilon}, \quad \boldsymbol{\varepsilon} \sim \rho N(\mathbf{0}, \text{diag}\{\boldsymbol{c}_i\}) + (1-\rho) N(\mathbf{0}, \tau \text{diag}\{\boldsymbol{c}_i\}),$$

and replace $\boldsymbol{\theta}_i^{[k]}$ in $\boldsymbol{\Theta}^{[k]}$ by $\boldsymbol{\theta}_i^p$ with probability $\min(\zeta_i, 1)$, where

$$\zeta_i = \frac{L(\boldsymbol{y} \,|\, \boldsymbol{\theta}_i^p, \boldsymbol{\Theta}_{-i}^{[k]})\, \pi(\boldsymbol{\theta}_i^p, \boldsymbol{\Theta}_{-i}^{[k]})}{L(\boldsymbol{y} \,|\, \boldsymbol{\Theta}^{[k]})\, \pi(\boldsymbol{\Theta}^{[k]})}.$$

Step 3. If $k < K_1$, go to Step 1.

Upon completion, these first K_1 iterations yield the burn-in sample. Following Chen et al. (2012), we set $\rho = 0.95$, $\tau = 100$, and tune the vectors of positive numbers $\boldsymbol{c}_i$ so that the empirical acceptance rate lies in the range $(0.2, 0.45)$. Tuning is done every 100 iterations by increasing each element in $\boldsymbol{c}_i$ when the acceptance rate in the last 100 iterations is higher than 0.45, or decreasing $\boldsymbol{c}_i$ when this rate is lower than 0.2.

At the end of the first K_1 iterations, the burn-in sample mean $\boldsymbol{\mu}_i$ and covariance matrix $\boldsymbol{\Sigma}_i$ of $\boldsymbol{\theta}_i$ with corresponding lower triangular Cholesky factor $\boldsymbol{\Sigma}_i^{1/2}$ are computed for $i = 1, 2, 3$. The MCMC sampling scheme then continues for K_2 additional iterations according to the following independent MH steps:

Step 4. Increment k by 1 and set $\boldsymbol{\Theta}^{[k]}$ equal to $\boldsymbol{\Theta}^{[k-1]}$.

Step 5. For $i = 1, 2, 3$ in turn, generate $\boldsymbol{\theta}_i^p$ as

$$\boldsymbol{\theta}_i^p = \boldsymbol{\mu}_i + \boldsymbol{\Sigma}_i^{1/2} \boldsymbol{\varepsilon}, \quad \boldsymbol{\varepsilon} \sim \rho N(\mathbf{0}, \boldsymbol{I}) + (1-\rho) N(\mathbf{0}, \tau \boldsymbol{I}),$$

and replace $\boldsymbol{\theta}_i^{[k]}$ in $\boldsymbol{\Theta}^{[k]}$ by $\boldsymbol{\theta}_i^p$ with probability $\min(\zeta_i, 1)$, where now

$$
\begin{aligned}
\zeta_i &= \frac{L(\boldsymbol{y} \mid \boldsymbol{\theta}_i^p, \boldsymbol{\Theta}_{-i}^{[k]})\, \pi(\boldsymbol{\theta}_i^p, \boldsymbol{\Theta}_{-i}^{[k]})\, q(\boldsymbol{\theta}_i^{[k]})}{L(\boldsymbol{y} \mid \boldsymbol{\Theta}^{[k]})\, \pi(\boldsymbol{\Theta}^{[k]})\, q(\boldsymbol{\theta}_i^p)}, \\
q(\boldsymbol{\theta}_i) &\propto \rho \exp\left\{-\frac{1}{2}\,(\boldsymbol{\theta}_i - \boldsymbol{\mu}_i)'\, \boldsymbol{\Sigma}_i^{-1}\, (\boldsymbol{\theta}_i - \boldsymbol{\mu}_i)\right\} \\
&\quad + \frac{(1-\rho)}{\tau^{\dim(\boldsymbol{\theta}_i)/2}} \exp\left\{-\frac{1}{2\tau}\,(\boldsymbol{\theta}_i - \boldsymbol{\mu}_i)'\, \boldsymbol{\Sigma}_i^{-1}\, (\boldsymbol{\theta}_i - \boldsymbol{\mu}_i)\right\}.
\end{aligned}
$$

Step 6. If $k < K_1 + K_2$, go to Step 4.

Observe that the use of $\boldsymbol{\Sigma}_i$ in Step 5 accounts for the posterior correlation among the elements of $\boldsymbol{\theta}_i$, thereby improving the efficiency of the Markov chain.

In the illustrations presented next we set $K_1 = 30,000$ for the burn-in sample and $K_2 = 30,000$ with a thinning of 2 for the second sample, resulting in posterior samples comprising 15,000 draws. The convergence of the second-step Markov chains is assessed in the empirical application using the Geweke (1992) test. For each parameter, we also assess the accuracy of its posterior mean by computing the numerical standard error (NSE) according to the batch-means method (Ripley, 1987).

4 Illustrations

Before we apply the proposed model to actual data, we first present in this section the results of some simulation experiments about the performance of the adaptive MCMC sampler for posterior inference with the UnGARCH model. The developed model is then illustrated with an empirical application to the daily returns on four major international stock market indices: the Standard & Poor's (S&P) 500 (US), the FTSE 100 (UK), the DAX (Germany), and the CAC 40 (France).

4.1 Simulation results

We consider the UnGARCH model specified in turn with the Frank, FGM, RC90, and RC270 copulas. The true model parameters were set to values close to the posterior means obtained with the S&P 500 returns, and we consider sample sizes $T = 1500$ and $T = 3000$. Starting the recursions at zero, we simulated 50,000 returns and retained only the last T to mitigate the effects of the initial values. To see how we simulate data from the UnGARCH model, consider the Frank copula as an example. Given the simulated returns and parameter values at time $t-1$, the next simulated return $\tilde{R}_t$ is obtained according to the following steps:

Step 1. Compute $\tilde{p}_t$, $\tilde{m}_{2,R_t}$, $\tilde{m}_{4,\varepsilon_t^*}$, $\tilde{\nu}_t$, $\tilde{\lambda}_t$, and $\tilde{\alpha}_t$.

Step 2. Draw $\tilde{z} \sim U[0,1]$ and let $|\tilde{\varepsilon}_t| = G^{-1}\left(\frac{\tilde{z}+1}{2}\right)$, where G^{-1} is the quantile function of a Student-t distribution with $\tilde{\nu}_t$ degrees of freedom

Step 3. Compute

$$\tilde{\varrho}_t = \begin{cases} \left(1 - \frac{1-e^{-\tilde{\alpha}_t(1-\tilde{p}_t)}}{1-e^{\tilde{\alpha}_t \tilde{p}_t}} e^{\tilde{\alpha}_t(1-\tilde{z})}\right)^{-1}, & \text{if } \tilde{\alpha}_t \neq 0, \\ \tilde{p}_t, & \text{if } \tilde{\alpha}_t = 0. \end{cases}$$

and set $\tilde{S}_t = \mathbb{I}[\tilde{u} < \tilde{\varrho}_t]$, where $\tilde{u} \sim U[0,1]$.

Step 4. Compute $\tilde{R}_t = \tilde{\lambda}_t |\tilde{\varepsilon}_t| (2\tilde{S}_t - 1)$.

These simulation steps exploit the structure of the joint density/mass function in (11). In particular, observe that $\Pr[\tilde{S}_t = 1] = \tilde{\varrho}_t$ in Step 3, which brings about the conditional dependence between $|\tilde{R}_t|$ and $\tilde{S}_t$. The other UnGARCH specifications simply use a different copula function in this step.

Table 1 reports the simulation results, where for each model parameter value we report the true value used to generate the data, the means (of the posterior means) as well as the root mean squared error (RMSE) across replications. The overall picture that emerges from Table 1 is that the estimates appear quite accurate.[1] We have also observed that in many cases the posterior distributions appear skewed but still with most of the density concentrated near the true parameter values. This can be gleaned from Table 1 by comparing the true parameter values with the average estimates. We see that the posterior means are relatively close on average to the true parameter values. The RMSEs indicate the relative accuracy of these estimates, which, as expected, improves as the sample size increases.

4.2 Empirical results

In this section, we apply the UnGARCH model to the daily returns on the S&P 500, FTSE 100, DAX, and CAC 40. Returns were defined as $100\log(P_t/P_{t-1})$, where P_t is the closing value of the index on day t, and these returns were computed over the sample period covering January 4, 1999 to October 12, 2012. Owing to different holidays, the resulting samples sizes vary slightly across countries so that $T = 3469$ (S&P 500), 3480 (FTSE 100), 3513 (DAX), 3525 (CAC 40). The time series of daily prices and log returns are shown in the top two panels of Figures 9–12, and some summary statistics are reported in Table 2. As usual, volatility clustering effects (typically associated with periods of falling security prices) can be seen from the time-series plots and the summary statistics reveal evidence of excess kurtosis in the unconditional distribution of returns. The unconditional distributions of S&P 500 and FTSE 100 returns appear negatively skewed, while those of the DAX and CAC 40 returns show a small degree of positive skewness.

[1] Additional evidence (available upon request) shows the convergence of the Markov chain. Our results indicated a good mixing performance with the Markov chain moving rather fluidly as it explored the parameter space.

4.2.1 Alternative models

For comparison purposes, we also include in our empirical application several other models that are close to our proposed specification. Recall that if returns are conditionally symmetric each time period, then the general UnGARCH specification collapses to the autoregressive conditional kurtosis model proposed by Brooks et al. (2005) in (13)–(17). The nested BBHP version of our model is therefore an interesting benchmark to see how well these restrictions hold in the data.[2]

We also consider the non-nested specification proposed by León et al. (2005) who model autoregressive conditional heteroskedasticity, skewness, and kurtosis by assuming a series expansion of the normal density function. As in White et al. (2012), the adopted LRS specification is given by

$$R_t = \sigma_t \varepsilon_t, \quad \varepsilon_t \,|\, \mathfrak{F}_{t-1} \sim GC_4(0,1), \tag{24}$$

$$\sigma_t^2 = \omega_0 + \omega_1 R_{t-1}^2 + \omega_2 \sigma_{t-1}^2, \tag{25}$$

$$s_t = \gamma_0 + \gamma_1 \frac{R_{t-1}^3}{\sigma_{t-1}^3} + \gamma_2 s_{t-1}, \tag{26}$$

$$k_t = \delta_0 + \delta_1 \frac{R_{t-1}^4}{\sigma_{t-1}^4} + \delta_2 k_{t-1}, \tag{27}$$

where $GC_4(0,1)$ is a Gram-Charlier density of order 4. This density is found by taking a Gram-Charlier series expansion of the standard normal density function and truncating at the fourth moment to obtain:

$$g_{\varepsilon_t}(x \,|\, \mathfrak{F}_{t-1}) = \phi(\varepsilon_t)\psi(\varepsilon_t),$$

$$\psi(\varepsilon_t) = 1 + \frac{s_t}{3!}(\varepsilon_t^3 - 3\varepsilon_t) + \frac{k_t - 3}{4!}(\varepsilon_t^4 - 6\varepsilon_t^2 + 3),$$

where $\phi(\cdot)$ is the standard normal probability density function. Observe that the function $g(\cdot)$ is not a well-defined density since it need not integrate to one and $\psi(\cdot)$ could be negative. In order to solve these problems, León et al. (2005) take the square of $\psi(\cdot)$ and then normalize it. The resulting conditional $GC_4(0,1)$ density function for ε_t takes the form:

$$f_{\varepsilon_t}(x \,|\, \mathfrak{F}_{t-1}) = \phi(x)\psi^2(x)/\Gamma_t,$$

$$\Gamma_t = 1 + \frac{s_t^2}{3!} + \frac{(k_t - 3)^2}{4!},$$

[2] The proposed UnGARCH model was further compared with the GARCH model of Bollerslev (1987), the GJR-GARCH model of Glosten et al. (1993), and the EGARCH model of Nelson (1991). In order to save space those results are not included here, but they remain available upon request.

which yields the conditional density of R_t in (24) as $f_{R_t}(x \mid \mathfrak{F}_{t-1}) = f_{\varepsilon_t}(x/\sigma_t \mid \mathfrak{F}_{t-1})/\sigma_t$. See Del Brio and Perote (2012) for a recent discussion and further references on Gram-Charlier densities.

Our UnGARCH model is a natural extension of Anatolyev and Gospodinov (2010) (AG) whereby we introduce the notion of a folded distribution while accommodating the idea of autoregressive conditional kurtosis, suggested by Brooks et al. (2005). Another interesting comparison is thus between the UnGARCH model and AG's original decomposition model, which does not explicitly account for a time-varying conditional kurtosis. The AG model also begins with the return decomposition in (2) but then specifies

$$|R_t| = \psi_t \frac{\eta_t}{\Gamma(1+\kappa^{-1})},$$

where the positive multiplicative error η_t follows a Weibull distribution with shape parameter $\kappa > 0$ (Anatolyev and Gospodinov, 2010, §3.3). The scaling by $\Gamma(1+\kappa^{-1})$ ensures that $E(|R_t| \mid \mathfrak{F}_{t-1}) = \psi_t$. This conditional expectation is parameterized as

$$\log(\psi_t) = \omega_0 + \omega_1 \log(|R_{t-1}|) + \omega_2 \log(\psi_{t-1}) \tag{28}$$

and, as before, the conditional distribution of S_t is $\mathcal{B}(p_t \mid \mathfrak{F}_{t-1})$ with p_t given by (10). We close the AG model by specifying the joint distribution for $(|R_t|, S_t)'$ exactly as we did in Section 2.2 for the UnGARCH model, i.e. $|R_t|$ and S_t are joined using copula functions (Frank, FGM, RC90, RC270) with parameter α_t governed by (12). We examine the original AG model with constant copula parameters (b_1, b_2 zero) and then we relax this restriction to allow for a time-varying conditional return skewness, as in the UnGARCH model. We use AG-Con and AG-TV, respectively, to denote these models.

The MCMC approach described in the previous section was used for all the competing models. Tables 3–8 report the estimation results for each model, where the entries are the posterior means of each parameter and the associated NSEs are shown in parentheses. The numbers in square brackets are the values of the Geweke (1992) test statistic. If the output of the Markov chain is compatible with stationarity, then this statistic follows a standard normal distribution. The generally insignificant values in Tables 3–8 indicate that convergence to the stationarity distribution was achieved.

Table 3 shows the estimation results for the BBHP and LRS models. The estimated parameters of the conditional variance processes in (15) and (25) are similar to what is typically obtained with heavy-tailed GARCH models.[3] The parameter estimates for the conditional kurtosis equations in (16) and (27), however, tell a different story. In the LRS specification, the parameter δ_1 on lagged

[3]The GARCH model with Student-t innovations shows that the persistence of shocks to volatility (as measured by the estimate of $\omega_1 + \omega_2$) is close to one, with the estimate of ω_2 (≈ 0.90) much greater than that of ω_1 (≈ 0.09). The estimates of the degrees-of-freedom parameter ν vary from about 5 to 13, which is comparable to the estimates obtained by Luger (2012) with classical methods.

fourth powers of the standardized returns is close to zero, while the parameter δ_2 on the lagged kurtosis coefficient is higher in value. On the contrary, the BBHP specification yields estimates of δ_1 larger than those of δ_2, which itself appears to play a role in the kurtosis equation. These findings are in line with those obtained by León et al. (2005) and Brooks et al. (2005). Turning to the conditional skewness equation in (26), we see a similar pattern as before: the estimate of γ_1 is close to zero, while that of γ_2 is larger, and again this finding agrees with León et al. (2005).

Tables 4–7 show the Bayesian estimation results with the UnGARCH model using the returns on the S&P 500, FTSE 100, DAX, and CAC 40, respectively. Focusing on the posterior means in these tables, we see that the parameter estimates of the conditional second moment m_{2,R_t} resemble those of the conditional variance σ_t^2 seen in Table 3 with the BBHP and LRS models. Indeed, we see that $\hat{\omega}_1 \approx 0.09$ and $\hat{\omega}_2 \approx 0.90$ across all four indices. We also notice that the parameter estimates of the conditional fourth moment m_{4,ε_t^*} are very close to those of the conditional kurtosis k_t in Table 3 for the corresponding return series. These findings are to be expected when the conditional mean of daily returns is close to zero. Observe also in Tables 4–7 that the estimates of the parameters describing the conditional second and fourth moments are quite similar across copula specifications. Again this is not surprising since the dependence between $|R_t|$ and S_t is expected to be weak if the returns tend to be only weakly conditionally asymmetric. Looking at the estimates of the parameters of p_t in (10), we see that they too are very similar across copula specifications. In this equation, the lagged squared return seems to play a small role, whereas the estimates of φ_2 and φ_3 tend to be much larger in magnitude and of opposite signs so that $\log(p_t/(1-p_t))$ depends negatively on S_{t-1}, and positively on its own lagged value. The posterior means of the parameters of the copula equation in (12) assign a lesser role to $|R_{t-1}|(1-S_{t-1})$ compared to the relatively greater one played by the lagged value of the copula parameter itself, in all copula specifications.

Figures 1–4 show the fitted conditional variance (volatility), skewness, and kurtosis series for the BBHP, LRS, and UnGARCH-Frank models and for each stock market index. The skewness and kurtosis plots exhibit large spikes in their values. This is to be expected given the definitions in (22) and (23) which show that the coefficients of skewness and kurtosis can become arbitrarily large, depending on how small σ_t in the denominator becomes. It is interesting to note that the large negative (positive) spike in skewness (kurtosis) in Figure 1 occurred on February 27, 2007, the day when HSBC Bank wrote down its holdings of subprime mortgage-backed securities, which was the first major subprime-related loss to be reported. In Figures 2–4, we also see a large negative (positive) spike in skewness (kurtosis) occurring on January 21, 2008 in the FTSE 100, DAX, and CAC 40 series. This was precisely when the French bank Société Générale lost 4.9 billion euros closing out positions that resulted from the allegedly unauthorized transactions of Jérôme Kerviel, a trader with Société Générale at the time (Reuters). The European stock markets were hit hard with the FTSE 100, DAX, and CAC 40 losing around 5 to 7% on that single day.

Table 8 reports the estimation results for the AG models with constant and time-varying Frank copulas.[4] The parameter estimates of the conditional expectation in (28) resemble those of a daily GARCH equation, i.e. the estimates of ω_1 are around 0.04 and the estimates of ω_2 are around 0.95. This is not surprising since absolute values depend on the variance of the distribution. For example, under normality we have $E(|R_t| \,|\, \mathfrak{F}_{t-1}) = \sigma_t\sqrt{2/\pi}$. Comparing each market at a time, we notice that the AG and UnGARCH models yield broadly consistent estimates for the dynamic logit model describing the dynamics of S_t, at least for the AG models with time-varying copulas. In the constant copula cases, it is interesting to note the generally negative values of $\hat{\alpha}$ which is indicative of negative skewness in the conditional return distribution. As an illustration, Figures 5–8 show the series of fitted volatility and conditional skewness from the AG models with a Frank copula applied to the S&P 500 returns. The apparent similarity between the volatilities of the AG-Con and AG-TV models is explained by the fact that the estimated copula parameter b_1 in (12) is quite small. This concurs with the evidence of weak serial dependence in the conditional skewness of returns already revealed in Figures 1–4 by the LRS and UnGARCH models.

In addition to the levels and returns of each stock market index, Figure 9–12 show the fitted series for: (i) the conditional mean, $E_{t-1}(R_t) = E(R_t \,|\, \mathfrak{F}_{t-1})$; (ii) the parameter α_t of the Frank copula; and (iii) the probability $p_t = \Pr(R_t > 0 \,|\, \mathfrak{F}_{t-1})$. In all four markets, we see that declining stock prices are accompanied by increased return volatility, higher values of α_t, and smaller values of p_t. Recall that α_t captures the dependence between $|R_t|$ and S_t, so that an increase in α_t corresponds to an increase in return skewness when all else is held constant. This finding of positive or less negative α_t being associated with lower stock prices is broadly consistent with the results of Conrad et al. (2013). But here we see that periods where return skewness would increase due to increasing α_t are offset by the decreasing p_t. The net effect on the conditional mean is different across markets. Looking at the S&P 500 and FTSE 100 around 2009 we see that $E_{t-1}(R_t)$ was more volatile but also holding at larger positive value for sustained periods, perhaps in anticipation of the market upturn. On the other hand, the DAX and CAC 40 reveal more negative values for $E_{t-1}(R_t)$ during that time.

4.2.2 Specification tests

A correct model specification translates into a set of conditional moment restrictions, which in turn means that their unconditional counterparts should hold true. Following Nelson (1991) and Brooks et al. (2005), we test for correct model specification by applying the tests of Newey (1985) to appropriately standardized returns. Of course, the appropriate standardization depends on the model used to filter the returns. Indeed if a return series is correctly filtered, then it should have mean zero, unit variance, and be free of serial correlation. Otherwise, the model is misspecified in some regard.

[4]The AG model estimation results with the other copulas are omitted.

As in Brooks et al. (2005), we test the model specifications by assessing nine moment conditions:

$$
\begin{aligned}
E[z_t] &= 0, \\
E[z_t z_{t-j}] &= 0, \text{ for } j = 1,2,3,4, \\
E\left[w_t w_{t-j}\right] &= 0, \text{ for } j = 1,2,3,4,
\end{aligned}
$$

where the standardized UnGARCH returns are

$$
z_t = |\varepsilon_t| - E(|\varepsilon_t|) = \frac{R_t}{(2S_t - 1)\lambda_t} - \frac{2D(\nu_t)\nu_t}{\nu_t - 1}, \tag{29}
$$

$$
w_t = \varepsilon_t^2 - \frac{\nu_t}{\nu_t - 2}, \tag{30}
$$

with the normalizing function

$$
D(\nu_t) = \frac{\Gamma\left(\frac{\nu_t+1}{2}\right)}{\Gamma\left(\frac{\nu_t}{2}\right)\sqrt{\pi\nu_t}},
$$

which follows from the properties of the folded Student-t distribution (Psarakis and Panaretos, 1990). Note that $D(\nu)$ is the normalizing constant of the usual Student-t density.

For the BBHP model in (13)–(17), the moment conditions are defined with

$$
z_t = \varepsilon_t = \frac{R_t}{\lambda_t},
$$

while w_t is still given by (30). When testing the LRS model in (24)–(27), we replace (29) and (30) by

$$
\begin{aligned}
z_t &= \varepsilon_t = \frac{R_t}{\sigma_t}, \\
w_t &= z_t^2 - 1,
\end{aligned}
$$

and for the AG model the returns are filtered according to

$$
\begin{aligned}
z_t &= \frac{\eta_t}{\Gamma(1+\kappa^{-1})} - 1 = \frac{R_t}{(2S_t - 1)\psi_t} - 1, \\
w_t &= \frac{\eta_t^2}{\Gamma(1+\kappa^{-1})^2} - \Gamma\left(1 + \frac{2}{\kappa}\right) / \Gamma\left(1 + \frac{1}{\kappa}\right)^2.
\end{aligned}
$$

The results of the moment specification tests are presented in Tables 9–12, where for each of the nine selected moment conditions the tables report the corresponding sample analogues as well as the test statistics in parenthesis. If the examined model has fully captured the dynamic features represented by the moment conditions, then the associated test statistics follow a $\chi^2(1)$ distribution; asterisks are used in the tables to denote cases of significance at the 5% and 1% levels. As expected, the findings vary a great deal across models and markets.

For the S&P 500 (Table 9), the tests statistics for $E[z_t z_{t-1}] = 0$ are significantly different from zero under each model specification. A similar result is found for the moment condition $E[w_t w_{t-1}] = 0$, except for the AG models which seem to pass this test. In sharp contrast, however, the AG models appear misspecified according to almost all the other moment conditions while the other models generally pass the specification tests. The evidence about the AG model failing to satisfy most of the moment criteria shows up also in Tables 10–12 with the FTSE 100, DAX, and CAC 40. Indeed, the AG model consistently fails five or more of the nine moment tests in these markets. The UnGARCH models seem to improve further upon the LRS and BBHP specifications. In the case of the FTSE 100 (Table 10), for instance, the UnGARCH is the only model to pass all specification tests. And with the CAC 40 (Table 12), the UnGARCH model with the Frank and RC90 copulas also passes unblemished. By looking simply at the total number of moment conditions satisfied over all four markets, we see that among all the model specifications the UnGARCH seems to best capture the features of the data.

Of course, the conditional moments tests may not detect all potential sources of misspecification. So after the formal model comparisons presented next, we also evaluate the out-of-sample forecasting performance of the competing models.

4.2.3 Model comparisons

In order to formally compare the different model specifications, we use the reversible jump MCMC (RJMCMC) method of So et al. (2005) and Chen et al. (2006) which they adapted from Green (1995) to the case of GARCH-type models. The RJ sampler can be viewed as an extension of the MH algorithm to more general state spaces. The RJMCMC method estimates posterior probabilities between pairs of competing models by allowing jumps between (possibly non-nested) models of different dimensions inside an MCMC sample. To explain the pairwise comparison method, let M_1 denote the LRS model and M_2 the UnGARCH-Frank model, for example. The parameters of M_1 are $\boldsymbol{\Theta}_1 = (\boldsymbol{\theta}_{11}, \boldsymbol{\theta}_{12}, \boldsymbol{\theta}_{13})$ with $\boldsymbol{\theta}_{11} = (\omega_0, \omega_1, \omega_2)$, $\boldsymbol{\theta}_{12} = (\gamma_0, \gamma_1, \gamma_2)$, and $\boldsymbol{\theta}_{13} = (\delta_0, \delta_1, \delta_2)$. The parameters of M_2 are $\boldsymbol{\Theta}_2 = (\boldsymbol{\theta}_{21}, \boldsymbol{\theta}_{22}, \boldsymbol{\theta}_{23})$ with $\boldsymbol{\theta}_{21} = (\omega_0, \omega_1, \omega_2, \delta_0, \delta_1, \delta_2)$, $\boldsymbol{\theta}_{22} = (\varphi_0, \varphi_1, \varphi_2, \varphi_3)$, and $\boldsymbol{\theta}_{23} = (b_0, b_1, b_2)$. As in Chen et al. (2006), we create a one-to-one bijective transformation between the two models by defining $\boldsymbol{u}_1 = \boldsymbol{\Theta}_2$ and $\boldsymbol{u}_2 = \boldsymbol{\Theta}_1$; see also Vrontos et al. (2002). This implies that the Jacobian determinant of the transformation from $(\boldsymbol{\Theta}_1, \boldsymbol{u}_1)$ to $(\boldsymbol{u}_2, \boldsymbol{\Theta}_2)$ equals 1, and it also ensures the necessary dimension-matching condition: $\dim(\boldsymbol{\Theta}_1) + \dim(\boldsymbol{u}_1) = \dim(\boldsymbol{u}_2) + \dim(\boldsymbol{\Theta}_2)$.

To apply the RJMCMC method we must choose prior probabilities of a jump from model M_i to M_j, denoted as $j(M_i, M_j)$. The output from the independent MH sampler can then be used to obtain a full probabilistic description of the posterior probabilities of each model, in addition to the posterior distributions of the individual model parameters. Specifically, after the first K_1 random walk MH burn-in steps, we start at $k = 1$ from model M_1 with initial parameters $\boldsymbol{\Theta}_1^{[1]}$ and the RJ sampler then proceeds along the following steps until k equals K_2:

Step 1. Generate $\mathbf{\Theta}_2^p$ in M_2 from the proposal density $q_1(\boldsymbol{u}_1)$, and accept the jump from M_1 to M_2 with probability $\min(\wp, 1)$, where

$$\wp = \frac{L(\boldsymbol{y}|M_2, \mathbf{\Theta}_2^p)\, \pi(\mathbf{\Theta}_2^p|M_2)\, p(M_2)\, j(M_1, M_2)\, q_2(\mathbf{\Theta}_1^{[k]})}{L(\boldsymbol{y}|M_1, \mathbf{\Theta}_1^{[k]})\, \pi(\mathbf{\Theta}_1^{[k]}|M_1)\, p(M_1)\, j(M_2, M_1)\, q_1(\mathbf{\Theta}_2^p)}.$$

Increment k by 1. If the jump from M_1 to M_2 was accepted, set $\mathbf{\Theta}_2^{[k]}$ equal to $\mathbf{\Theta}_2^p$ and go to Step 2. Otherwise, update $\mathbf{\Theta}_1^{[k-1]}$ to $\mathbf{\Theta}_1^{[k]}$ within M_1 according to the independent MH scheme and go to Step 1.

Step 2. Generate $\mathbf{\Theta}_1^p$ in M_1 from the proposal density $q_2(\boldsymbol{u}_2)$, and accept the reverse jump from M_2 back to M_1 with probability $\min(\wp, 1)$, where now

$$\wp = \frac{L(\boldsymbol{y}|M_1, \mathbf{\Theta}_1^p)\, \pi(\mathbf{\Theta}_1^p|M_1)\, p(M_1)\, j(M_2, M_1)\, q_1(\mathbf{\Theta}_2^{[k]})}{L(\boldsymbol{y}|M_2, \mathbf{\Theta}_2^{[k]})\, \pi(\mathbf{\Theta}_2^{[k]}|M_2)\, p(M_2)\, j(M_1, M_2)\, q_2(\mathbf{\Theta}_1^p)}.$$

Increment k by 1. If the jump from M_2 to M_1 was accepted, set $\mathbf{\Theta}_1^{[k]}$ equal to $\mathbf{\Theta}_1^p$ and go to Step 1. Otherwise, update $\mathbf{\Theta}_2^{[k-1]}$ to $\mathbf{\Theta}_2^{[k]}$ within M_2 according to the independent MH scheme and go to Step 2.

Upon completion, the number of times out of K_2 that each model is chosen provides an estimate of its posterior probability, $\Pr(M_i|\boldsymbol{y})$. Here we set $j(M_1, M_2) = j(M_2, M_1) = 1$ to allow jumps between models at each iteration. The priors $\pi(\mathbf{\Theta}_i|M_i)$ appearing in the expressions for $\wp$ are again taken as uniform over their respective parameter spaces, and we set the prior model probabilities as $p(M_i) = 1/2$, $i = 1, 2$. Following Chen et al. (2006), the joint proposal densities $q_i(\boldsymbol{u}_i)$ are chosen as the product of the independent normal proposal distributions built up during the first K_1 random walk MH steps. See Hastie and Green (2012) for a recent and more detailed presentation of the RJMCMC method.

Table 13 presents the estimated posterior model probabilities of the models listed in the column heading versus each model listed on the rows, in turn. So with the S&P 500 returns for example, the UnGARCH-Frank model has a posterior probability estimate of 0.85 when compared to the UnGARCH-FGM model. We see immediately that the UnGARCH models are strongly preferred to the AG models, with posterior model probabilities of 1. The UnGARCH specifications are also generally preferred to the LRS and BBHP models. The notable exceptions occur when the RC270 copula is used, which tends to find far less support relative to the other competing models. Indeed, with FTSE 100, DAX, and CAC 40 returns, the UnGARCH-RC270 versus LRS comparison yields posterior probabilities of only 0.03, 0.06, and 0.18, respectively; and UnGARCH-RC270 versus BBHP yields 0.09, 0.10, 0.08, respectively.

These findings clearly show that the choice of copula matters for UnGARCH model selection. With these data, the general conclusion is that there is little support for tail dependence in the fourth quadrant. Among the UnGARCH specifications, the Frank copula, closely followed by the FGM copula, which both allow positive and negative dependence, seems to find the strongest support across all four markets.

4.2.4 Out-of-sample forecasting results

In this section we evaluate the out-of-sample forecasting performance of the competing models. Specifically, we examine their ability to predict the conditional mean and quantiles of the one-day-ahead return distribution. The forecasts are obtained using a rolling data window of size 2000 and updating the model parameter estimates every month, which leaves the period from July 2, 2007 to October 12, 2012 for evaluation.[5]

Conditional mean predictions. A distinguishing feature of the AG and UnGARCH models is that they both predict a time-varying conditional mean $\mu_t = E(R_t \,|\, \mathfrak{F}_{t-1})$, which corresponds to the optimal forecast of R_t under a quadratic loss function. It is therefore interesting to compare the return forecasts from these models. Table 14 shows the out-of-sample forecasting results under both quadratic and absolute loss functions. Specifically, we report losses relative to the "no change" benchmark associated with a random walk model of asset prices, so that a ratio less (greater) than 1 indicates that a model has a smaller (larger) loss than the benchmark. We see that the models actually have ratios close to one, which is not very surprising as daily returns have a conditional mean that does not deviate far from zero. Nevertheless, the UnGARCH models seem to perform slightly better than their AG counterparts. Indeed, the UnGARCH-Frank specification achieves the smallest losses on average across the four markets.

We formally tested these out-of-sample predictions in the context of a standard Mincer-Zarnowitz regression (Mincer and Zarnowitz, 1969) taking the form

$$R_t = a_0 + a_1 \hat{\mu}_t + \epsilon_t,$$

where R_t is the actual market return at time t and $\hat{\mu}_t$ is the conditional mean return predicted at time $t-1$. If the forecasts are unbiased, then $a_0 = 0$ and $a_1 = 1$. Table 15 reports the results for the variety of AG and UnGARCH models. The AG specifications appear at odds with the unbiasedness hypothesis. Indeed, 21 of the 32 AG models have p-values $\leq 5\%$. In sharp contrast, only 3 of the 16 UnGARCH models (UnGARCH-RC270 with S&P 500, FTSE 100, and CAC 40 returns) reject the null hypothesis at this level.

Value-at-risk predictions. The Basel II Accord on banking regulations specifies the value-at-risk (VaR) as the preferred measure of market risk for calculating minimum capital requirements. For a

[5] Following standard practice, the estimates are based on the posterior means. Even though this approach is efficient, it ignores the parameter uncertainty captured by the rest of the posterior distribution.

given probability level and a certain time horizon, the VaR of a portfolio is defined as the threshold value such that the loss suffered by the portfolio over the given horizon will only exceed it with the stated probability. For example, if p denotes the probability level, then the one-day VaR on a long position is defined via

$$\Pr\left(R_t \leq VaR_t^p \,|\, \mathfrak{F}_{t-1}\right) = p,$$

which makes clear that the VaR_t^p corresponds to the $p\,100\%$ conditional quantile of R_t. We use each of the competing models to forecast VaR_t^p over the evaluation period setting $p = 1\%, 5\%$. The VaR forecasts are obtained analytically for the BBHP model, whereas Monte Carlo simulations are used with the LRS, AG, and UnGARCH models to obtain the one-day-ahead conditional return distributions.

A commonly used criterion to compare VaR models is the violation rate $\hat{p}$, defined as the number of VaR exceedances (violations) divided by the evaluation sample size. The VaR forecasting performances are summarized by reporting the ratios $\hat{p}/p$ for each model, which ideally should be close to one. Otherwise if $\hat{p}/p < 1$, then loss estimates are too conservative (higher than actual), while a ratio $\hat{p}/p > 1$ means that actual losses are underestimated. Table 16 shows the results, where the entries in bold indicate the model whose ratio $\hat{p}/p$ is closest to one. The results depend on the nominal p. Indeed, for $p = 0.05$ the violation ratio of the BBHP model comes closest to one, while for the more extreme value $p = 0.01$ the best model is the UnGARCH-RC90. It is interesting to observe the consistency of these performances across the four markets. We further assess the VaR forecasts with the unconditional coverage (UC) test of Kupiec (1995), the conditional coverage (CC) test of Christoffersen (1998), and the dynamic quantile (DQ) test of Engle and Manganelli (2004) using four lags. These tests are quite standard in the VaR forecast evaluation literature; see Kuester et al. (2006) for details. Following Gerlach et al. (2011), we summarize the test outcomes in Table 17 by reporting the number of test rejections at the 5% significance level over the four markets. Here the bold entries indicate the model achieving the lowest number of rejections. The UnGARCH-RC90 specification is seen to perform remarkably well, with only three rejections across markets and values of p.

We next investigate the economic significance of the various models by comparing their implied capital charges under the Basel Accord. For model comparison purposes, we follow McAleer and da Veiga (2008) and da Veiga et al. (2012) and compute the market risk capital charges according to

$$cc^* = \min\left(cc(3+k), VaR_{t-1}^{0.01}\right),$$

where $cc = \frac{1}{60}\sum_{i=1}^{60} VaR_{t-i}^{0.01}$ is the average 1% VaR over the last 60 days. The multiplicative factor k is a penalty imposed when the number of VaR violations (over the last 250 days) becomes excessive. The specific values for each "penalty zone" are given in Table 18. A bank falling in the green zone is deemed to have an adequate model and does not incur a penalty. Once in the yellow zone, however, banks are required to hold more capital in reserve as protection against losses in their trading portfolios. If a bank's internal model results in too many VaR violations and enters the red zone, regulators may require the bank to adopt a standardized approach which can lead to even higher capital charges. Obviously, a high capital charge is undesirable as it reduces profitability. It is important to note that the capital charge calculation depends on both the penalty and the forecasted VaR.

The results of the regulatory backtesting are summarized in Table 19. For each model and market, we report the average capital charge and penalty incurred over the last 250 trading days, as well as the proportion of time spent in each penalty zone. Due to the initial window of size 250, these backtesting results cover the period from June 2, 2008 to October 12, 2012 (about 1100 trading days). For the S&P 500, the UnGARCH models yield the lowest capital charges. Among these, the UnGARCH-RC90 specification performs remarkably well with an average penalty of 0.17 and VaR forecasts falling in the green zone 60% of the time.

In the case of the FTSE 100, the UnGARCH-Frank model achieves the lowest capital charge (10.95) with VaR forecasts comfortably falling in the green zone 69% of the time and never in the red zone. The UnGARCH models are clearly favoured by the DAX returns. For instance, the UnGARCH-FGM model delivers an average capital charge of 11.97 while spending 93% of the time in the green zone. Finally, with the CAC 40, the VaR forecasts from the UnGARCH specifications with rotated Clayton copulas are 98% of the time in the green zone, while the resulting average capital charges are among the lowest attained by all the models.

5 Conclusion

This paper has proposed a new and flexible GARCH-type model for autoregressive conditional higher moments based on a decomposition of returns into their signs and absolute values. The approach combines models for the marginal distributions of signs and absolute values, and a copula for their interaction. The novelty of this approach is that return skewness is determined via the copula function, which may evolve separately over time from the conditional kurtosis itself determined through the degrees of freedom of the folded Student-t distribution. Under the independence copula structure, the model reduces to the autoregressive conditional kurtosis specification of Brooks et al. (2005). Furthermore, if the degrees-of-freedom parameter is constant, then the model becomes a GARCH specification *à la* Bollerslev (1987). The conditional expectation of returns under the proposed copula approach may vary over time, since it is determined by the interaction between the signs and absolute values of returns.

We adopted a Bayesian approach using MCMC sampling for estimation and inference. This choice was motivated by the fact that the likelihood function is rather complicated and not everywhere differentiable owing to the presence of the absolute value and indicator functions. We found that a Bayesian approach with non-informative priors gave satisfactory results. We also illustrated the proposed UnGARCH model along with a host of alternative specifications through an application to the daily returns on four major international stock market indices for the period from January 4, 1999 to October 12, 2012. The results of in-sample conditional moment tests show that among all the considered models the UnGARCH seems to best capture the features of the daily returns. A formal Bayesian in-sample model comparison further shows that the new model is generally favoured over the competing models. The results obtained with the new copula model reveal interesting patterns for the model-implied conditional expectation of returns, particularly during the recent global financial crisis.

The out-of-sample analysis demonstrated that the UnGARCH model for conditional higher moments offers forecasting improvements over the competing specifications. Specifically, we examined the predictive ability of the time-varying conditional mean from the new model using standard Mincer-Zarnowitz regressions, and the forecasts were found to be generally compatible with the unbiasedness hypothesis. We also illustrated the economic significance of the various models with a risk management application focused on value-at-risk forecasting. The results of a regulatory backtesting exercise show that the proposed UnGARCH model improves upon the other competing models by yielding low average capital charges while being subject to relatively fewer penalties.

References

Almeida, C., Czado, C., 2012. Efficient Bayesian inference for stochastic time-varying copula models. Computational Statistics and Data Analysis 56, 1511–1527.

Anatolyev, S., Gospodinov, N., 2010. Modeling financial return dynamics via decomposition. Journal of Business and Economic Statistics 28, 232–245.

Ausin, M., Lopes, H., 2010. Time-varying joint distribution through copulas. Computational Statistics and Data Analysis 54, 2383–2399.

Bauwens, L., Lubrano, M., 1998. Bayesian inference on GARCH models using the Gibbs sampler. Econometrics Journal 1, C23–C46.

Bollerslev, T., 1987. A conditionally heteroskedastic time series model for speculative prices and rates of return. Review of Economics and Statistics 69, 542–547.

Brooks, C., Burke, S., Hearvi, S., Persand, G., 2005. Autoregressive conditional kurtosis. Journal of Financial Econometrics 3, 399–421.

Chen, C., Gerlach, R., So, M., 2006. Comparison of nonnested asymmetric heteroskedastic models. Computational Statistics and Data Analysis 51, 2164–2178.

Chen, Q., Gerlach, R., Lu, Z., 2012. Bayesian value-at-risk and expected shortfall forecasting via the asymmetric Laplace distribution. Computational Statistics and Data Analysis 56, 3498–3516.

Chib, S., Greenberg, E., 1995. Understanding the Metropois-Hastings algorithm. American Statistician 49, 327–335.

Christoffersen, P., 1998. Evaluating interval forecasts. International Economic Review 39, 841–862.

Christoffersen, P., Diebold, F., 2006. Financial asset returns, direction-of-change forecasting, and volatility dynamics. Management Science 52, 1273–1287.

Conrad, J., Dittmar, R., Ghysels, E., 2013. Ex ante skewness and expected stock returns. Journal of Finance 68, 85–124.

da Veiga, B., Chan, F., McAleer, M., 2012. It pays to violate: how effective are the Basel accord penalties in encouraging risk management? Accounting and Finance 52, 95–116.

de Jong, R., Woutersen, T., 2011. Dynamic time series binary choice. Econometric Theory 27, 673–702.

Del Brio, E., Perote, J., 2012. Gram-Charlier densities: maximum likelihood versus the method of moments. Insurance: Mathematics and Economics 51, 531–537.

Engle, R., Manganelli, S., 2004. CAViaR: Conditional autoregressive value at risk by regression quantiles. Journal of Business and Economic Statistics 22, 367–381.

Gerlach, R., Chen, C., Chan, N., 2011. Bayesian time-varying quantile forecasting for value-at-risk in financial markets. Journal of Business and Economic Statistics 29, 481–492.

Geweke, J., 1988. Exact inference in models with autoregressive conditional heteroscedasticity. In: Barnett, W., Berndt, E., White, H. (Eds.), Dynamic Econometric Modeling. Cambridge University Press, Cambridge, pp. 73–104.

Geweke, J., 1989. Exact predictive densities in linear models with ARCH disturbances. Journal of Econometrics 40, 63–86.

Geweke, J., 1992. Evaluating the accuracy of sampling-based approaches to calculating posterior moments. In: Bernardo, J., Berger, J., Dawid, A., Smith, A. (Eds.), Bayesian Statistics. Vol. 4. Oxford University Press, Oxford, pp. 169–193.

Glosten, L., Jagannathan, R., Runkle, D., 1993. On the relation between the expected value and the volatility of the nominal excess return on stocks. Journal of Finance 48, 1779–1801.

Green, P., 1995. Reversible jump MCMC computation and Bayesian model determination. Biometrika 82, 711–732.

Hansen, B., 1994. Autoregressive conditional density estimation. International Economic Review 35, 705–730.

Harvey, C., Siddique, A., 1999. Autoregressive conditional skewness. Journal of Financial and Quantitative Analysis 34, 465–487.

Hastie, D., Green, P., 2012. Model choice using reversible jump Markov chain Monte Carlo. Statistica Neerlandica 66, 309–338.

Jondeau, E., Poon, S.-H., Rockinger, M., 2007. Financial Modeling Under Non-Gaussian Distributions. Springer-Verlag, London.

Jondeau, E., Rockinger, M., 2003. Conditional volatility, skewness, and kurtosis: existence, persistence, and comovements. Journal of Economic Dynamics and Control 27, 1699–1737.

Kuester, K., Mittnik, S., Paolella, M., 2006. Value-at-risk prediction: a comparison of alternative strategies. Journal of Financial Econometrics 4, 53–89.

Kupiec, P., 1995. Techniques for verifying the accuracy of risk measurement models. Journal of Derivatives 3, 73–84.

León, A., Rubio, G., Serna, G., 2005. Autoregressive conditional volatility, skewness and kurtosis. Quarterly Review of Economics and Finance 45, 599–618.

Leone, F., Nelson, L., Nottingham, R., 1961. The folded normal distribution. Technometrics 3, 543–550.

Luger, R., 2012. Finite-sample bootstrap inference in GARCH models with heavy-tailed innovations. Computational Statistics and Data Analysis 56, 3198–3211.

Manner, H., Reznikova, O., 2012. A survey on time-varying copulas: specification, simulations, and application. Econometric Reviews 31, 654–687.

McAleer, M., da Veiga, B., 2008. Forecasting value-at-risk with a parsimonious portfolio spillover GARCH (PS-GARCH) model. Journal of Forecasting 27, 1–19.

Mincer, J., Zarnowitz, V., 1969. The evaluation of economic forecasts. In: Mincer, J. (Ed.), Economics Forecasts and Expectations: Analyses of Forecasting Behavior and Performance. Columbia University Press, New York, pp. 3–46.

Nelson, D., 1991. Conditional heteroskedasticity in asset returns: a new approach. Econometrica 59, 347–370.

Newey, W., 1985. Generalized method of moments specification testing. Journal of Econometrics 29, 229–256.

Patton, A., 2012. A review of copula models for economic time series. Journal of Multivariate Analysis 110, 4–18.

Psarakis, S., Panaretos, J., 1990. The folded t distribution. Communications in Statistics A, Theory and Methods 19, 2717–2734.

Randles, R., Wolfe, D., 1979. Introduction to the Theory of Nonparametric Statistics. Wiley, New York.

Ripley, B., 1987. Stochastic Simulation. John Wiley, New York.

So, M., Chen, C., Chen, M.-T., 2005. A Bayesian threshold nonlinearity test for financial time series. Journal of Forecasting 24, 61–75.

Trivedi, P., Zimmer, D., 2005. Copula modeling: an introduction for practitioners. Foundations and Trends in Econometrics 1, 1–111.

Vrontos, I., Dellaportas, P., Politis, D., 2002. Full Bayesian inference for GARCH and EGARCH models. Journal of Business and Economic Statistics 18, 187–198.

White, H., Kim, T.-H., Managanelli, S., 2012. Modeling autoregressive conditional skewness and kurtosis with multi-quantile CAViaR. In: Bollerslev, T., Russell, J., Watson, M. (Eds.), Volatility and Time Series Econometrics: Essays in Honor of Robert F. Engle. Oxford University Press, Oxford, pp. 231–256.

Table 1. Simulation results for the UnGARCH model

	Frank copula			FGM copula			RC90 copula			RC270 copula		
	True	Mean	RMSE	True	Mean	RMSE	True	Mean	RMSE	True	Mean	RMSE
Panel A: $T = 1500$												
ω_0	0.014	0.019	0.005	0.014	0.021	0.007	0.014	0.020	0.006	0.014	0.023	0.009
ω_1	0.090	0.099	0.009	0.090	0.099	0.009	0.090	0.097	0.007	0.090	0.100	0.010
ω_2	0.900	0.885	0.014	0.900	0.883	0.016	0.900	0.888	0.012	0.900	0.881	0.019
δ_0	3.400	3.794	0.394	3.400	3.796	0.396	3.400	3.701	0.301	3.400	3.647	0.247
δ_1	0.750	0.596	0.154	0.750	0.599	0.151	0.750	0.608	0.141	0.750	0.594	0.155
δ_2	0.060	0.090	0.031	0.060	0.090	0.030	0.060	0.096	0.035	0.060	0.097	0.037
φ_0	0.200	0.231	0.031	0.200	0.245	0.045	0.200	0.234	0.034	0.200	0.261	0.072
φ_1	-0.003	-0.019	0.017	-0.003	-0.029	0.027	-0.003	-0.016	0.013	-0.003	-0.017	0.014
φ_2	-0.250	-0.266	0.016	-0.250	-0.273	0.022	-0.250	-0.278	0.028	-0.250	-0.301	0.210
φ_3	0.325	0.293	0.041	0.325	0.299	0.025	0.325	0.292	0.033	0.325	0.301	0.025
b_0	-0.150	-0.206	0.057	-0.150	-0.221	0.071	-0.050	-0.066	0.016	-0.050	-0.011	0.044
b_1	0.150	0.233	0.083	0.150	0.213	0.063	-0.050	-0.056	0.006	-0.050	-0.012	0.043
b_2	0.400	0.312	0.087	0.400	0.345	0.054	0.400	0.319	0.080	0.400	0.287	0.112
Panel B: $T = 3000$												
ω_0	0.014	0.016	0.002	0.014	0.017	0.003	0.014	0.016	0.002	0.014	0.017	0.003
ω_1	0.090	0.095	0.005	0.090	0.096	0.006	0.090	0.095	0.005	0.090	0.096	0.006
ω_2	0.900	0.892	0.007	0.900	0.891	0.009	0.900	0.892	0.007	0.900	0.890	0.009
δ_0	3.400	3.431	0.031	3.400	3.395	0.004	3.400	3.467	0.067	3.400	3.390	0.009
δ_1	0.750	0.605	0.144	0.750	0.618	0.131	0.750	0.612	0.137	0.750	0.607	0.143
δ_2	0.060	0.078	0.019	0.060	0.077	0.023	0.060	0.079	0.021	0.060	0.082	0.024
φ_0	0.200	0.220	0.020	0.200	0.215	0.015	0.200	0.218	0.018	0.200	0.234	0.026
φ_1	-0.003	-0.012	0.010	-0.003	-0.014	0.011	-0.003	-0.011	0.009	-0.003	-0.009	0.006
φ_2	-0.250	-0.257	0.007	-0.250	-0.251	0.001	-0.250	-0.256	0.005	-0.250	-0.211	0.183
φ_3	0.325	0.298	0.032	0.325	0.295	0.023	0.325	0.294	0.031	0.325	0.319	0.005
b_0	-0.150	-0.188	0.038	-0.150	-0.184	0.034	-0.050	-0.059	0.009	-0.050	-0.059	0.038
b_1	0.150	0.208	0.058	0.150	0.181	0.031	-0.050	-0.052	0.001	-0.050	-0.067	0.038
b_2	0.400	0.327	0.073	0.400	0.338	0.061	0.400	0.318	0.082	0.400	0.288	0.111

Notes: For each model parameter, this table reports the true values used to generate the data, the mean across replications of the posterior means, and the root mean squared error (RMSE). The results are based on 100 replications of each data generating process.

Table 2. Summary statistics of daily log-returns (in percentages)

	Mean	Std. Dev.	Max	Min	Skewness	Kurtosis
S&P 500	0.004	1.342	10.957	-9.469	-0.151	10.064
FTSE 100	-0.001	1.291	9.384	-9.264	-0.119	8.418
DAX	0.011	1.613	10.797	-7.433	0.030	6.808
CAC 40	-0.004	1.553	10.595	-9.472	0.029	7.468

Table 3. Estimation results for the BBHP and LRS models

Model	ω_0	ω_1	ω_2	δ_0	δ_1	δ_2	γ_0	γ_1	γ_2
Panel A: S&P 500 returns									
BBHP	0.013	0.090	0.904	3.334	0.731	0.063			
	(0.005)	(0.011)	(0.010)	(0.106)	(0.084)	(0.017)			
	[-0.422]	[-0.725]	[0.812]	[-0.706]	[-0.163]	[-0.041]			
LRS	0.016	0.088	0.901	2.510	0.003	0.260	-0.067	0.008	0.228
	(0.006)	(0.018)	(0.016)	(0.193)	(0.004)	(0.530)	(0.015)	(0.004)	(0.073)
	[-0.480]	[0.101]	[-0.190]	[-0.498]	[-0.282]	[0.528]	[-1.247]	[-0.862]	[-0.969]
Panel B: FTSE 100 returns									
BBHP	0.017	0.114	0.879	2.801	0.474	0.123			
	(0.001)	(0.002)	(0.002)	(0.016)	(0.006)	(0.009)			
	[0.650]	[0.397]	[-0.349]	[-1.508]	[-0.446]	[1.916]			
LRS	0.015	0.101	0.889	2.981	0.002	0.055	-0.049	0.002	0.558
	(0.004)	(0.005)	(0.006)	(0.008)	(0.001)	(0.004)	(0.012)	(0.001)	(0.035)
	[1.846]	[1.423]	[-2.337]	[0.555]	[0.361]	[-2.654]	[-0.972]	[-0.553]	[-1.518]
Panel C: DAX returns									
BBHP	0.022	0.095	0.899	3.093	0.675	0.042			
	(0.006)	(0.007)	(0.008)	(0.040)	(0.035)	(0.019)			
	[0.068]	[-0.129]	[0.154]	[-0.645]	[0.321]	[1.239]			
LRS	0.022	0.083	0.907	2.778	0.009	0.122	-0.056	0.002	0.350
	(0.008)	(0.006)	(0.008)	(0.058)	(0.006)	(0.032)	(0.011)	(0.004)	(0.029)
	[0.274]	[-0.259]	[0.354]	[0.201]	[-1.786]	[-0.160]	[-0.875]	[0.727]	[-0.519]
Panel D: CAC 40 returns									
BBHP	0.021	0.094	0.901	2.470	0.553	0.229			
	(0.006)	(0.008)	(0.009)	(0.043)	(0.024)	(0.021)			
	[0.475]	[-0.551]	[0.364]	[-0.283]	[0.443]	[0.297]			
LRS	0.021	0.086	0.905	2.554	0.004	0.199	-0.097	0.001	-0.187
	(0.010)	(0.014)	(0.015)	(0.099)	(0.005)	(0.055)	(0.030)	(0.009)	(0.105)
	[0.994]	[1.393]	[-2.095]	[2.372]	[1.324]	[-0.306]	[-0.856]	[-1.294]	[-0.408]

Notes: This table reports the posterior means of each parameter, and the associated NSEs are shown in parentheses. The numbers in square brackets are the values of the Geweke (1992) convergence test statistic.

Table 4. Estimation results for the UnGARCH models with S&P 500 returns

ω_0	ω_1	ω_2	δ_0	δ_1	δ_2	φ_0	φ_1	φ_2	φ_3	b_0	b_1	b_2
Panel A: Frank copula												
0.013	0.092	0.902	3.335	0.729	0.068	0.204	-0.003	-0.252	0.332	-0.296	0.264	0.401
(0.005)	(0.005)	(0.006)	(0.082)	(0.051)	(0.021)	(0.016)	(0.002)	(0.023)	(0.039)	(0.029)	(0.038)	(0.039)
[−0.117]	[-0.142]	[0.258]	[-1.557]	[-1.214]	[0.901]	[-1.063]	[0.839]	[1.093]	[0.890]	[1.211]	[0.426]	[1.261]
Panel B: FGM copula												
0.013	0.090	0.904	3.337	0.745	0.061	0.203	-0.003	-0.251	0.327	-0.146	0.126	0.401
(0.006)	(0.009)	(0.010)	(0.097)	(0.058)	(0.024)	(0.011)	(0.003)	(0.017)	(0.036)	(0.018)	(0.018)	(0.035)
[0.305]	[0.500]	[-0.374]	[-0.167]	[-1.251]	[0.718]	[1.517]	[-1.534]	[-1.385]	[-0.345]	[−0.945]	[1.016]	[0.728]
Panel C: RC90 copula												
0.013	0.091	0.902	3.178	0.720	0.086	0.210	-0.002	-0.256	0.344	-0.069	0.004	0.337
(0.005)	(0.008)	(0.008)	(0.092)	(0.045)	(0.030)	(0.022)	(0.005)	(0.021)	(0.044)	(0.012)	(0.010)	(0.040)
[0.731]	[0.718]	[-0.771]	[-1.538]	[-0.445]	[1.321]	[0.158]	[0.423]	[-0.401]	[0.372]	[0.901]	[-0.336]	[1.448]
Panel D: RC270 copula												
0.013	0.090	0.903	3.323	0.772	0.056	0.204	-0.001	-0.242	0.309	-0.032	-0.006	0.323
(0.005)	(0.008)	(0.009)	(0.083)	(0.074)	(0.027)	(0.019)	(0.003)	(0.019)	(0.035)	(0.012)	(0.004)	(0.037)
[0.746]	[0.324]	[-0.369]	[0.024]	[0.551]	[-0.425]	[0.339]	[-1.347]	[-1.016]	[0.213]	[−0.396]	[1.744]	[-0.742]

Notes: This table reports the posterior means of each parameter, and the associated NSEs are shown in parentheses. The numbers in square brackets are the values of the Geweke (1992) convergence test statistic.

Table 5. Estimation results for the UnGARCH model with FTSE 100 returns

ω_0	ω_1	ω_2	δ_0	δ_1	δ_2	φ_0	φ_1	φ_2	φ_3	b_0	b_1	b_2
Panel A: Frank copula												
0.016	0.112	0.882	2.743	0.475	0.137	0.092	0.003	-0.143	0.406	-0.041	0.071	0.319
(0.007)	(0.013)	(0.013)	(0.108)	(0.088)	(0.056)	(0.017)	(0.008)	(0.025)	(0.037)	(0.025)	(0.026)	(0.029)
[0.905]	[-1.048]	[0.403]	[-0.443]	[-0.745]	[0.856]	[-1.691]	[1.105]	[1.204]	[-1.053]	[1.663]	[-1.022]	[0.202]
Panel B: FGM copula												
0.016	0.112	0.881	3.057	0.459	0.056	0.091	0.003	-0.142	0.403	-0.018	0.036	0.317
(0.008)	(0.012)	(0.013)	(0.066)	(0.068)	(0.021)	(0.018)	(0.006)	(0.027)	(0.045)	(0.016)	(0.019)	(0.050)
[−0.566]	[-0.592]	[0.378]	[-1.013]	[-0.329]	[0.325]	[1.856]	[-0.275]	[-0.216]	[1.527]	[0.479]	[-0.254]	[-0.631]
Panel C: RC90 copula												
0.017	0.113	0.881	2.807	0.516	0.116	0.096	0.003	-0.153	0.452	-0.043	-0.008	0.322
(0.005)	(0.014)	(0.014)	(0.129)	(0.072)	(0.069)	(0.015)	(0.004)	(0.025)	(0.042)	(0.012)	(0.011)	(0.026)
[0.235]	[-1.561]	[1.066]	[0.035]	[-1.735]	[0.005]	[-0.051]	[0.404]	[0.303]	[-1.069]	[−0.371]	[1.022]	[-0.008]
Panel D: RC270 copula												
0.016	0.114	0.879	2.751	0.458	0.134	0.096	0.003	-0.151	0.435	-0.008	-0.010	0.301
(0.004)	(0.011)	(0.011)	(0.145)	(0.069)	(0.078)	(0.017)	(0.004)	(0.017)	(0.043)	(0.008)	(0.008)	(0.039)
[−0.025]	[-1.191]	[1.021]	[-0.126]	[-0.239]	[0.147]	[-0.729]	[0.677]	[0.815]	[-0.598]	[−0.304]	[-1.406]	[0.677]

Notes: This table reports the posterior means of each parameter, and the associated NSEs are shown in parentheses. The numbers in square brackets are the values of the Geweke (1992) convergence test statistic.

Table 6. Estimation results for the UnGARCH model with DAX returns

ω_0	ω_1	ω_2	δ_0	δ_1	δ_2	φ_0	φ_1	φ_2	φ_3	b_0	b_1	b_2
Panel A: Frank copula												
0.021	0.094	0.901	2.988	0.655	0.066	0.128	-0.002	-0.108	0.366	-0.149	0.026	0.303
(0.009)	(0.013)	(0.074)	(0.122)	(0.067)	(0.045)	(0.019)	(0.003)	(0.026)	(0.039)	(0.033)	(0.027)	(0.041)
[−0.864]	[-0.587]	[0.429]	[-0.025]	[-0.527]	[-0.001]	[-0.836]	[-0.126]	[1.509]	[-0.191]	[−0.106]	[0.585]	[1.398]
Panel B: FGM copula												
0.022	0.095	0.899	3.006	0.690	0.062	0.127	-0.002	-0.105	0.353	-0.071	0.008	0.317
(0.006)	(0.008)	(0.041)	(0.053)	(0.027)	(0.016)	(0.021)	(0.007)	(0.025)	(0.055)	(0.018)	(0.021)	(0.034)
[−0.612]	[1.215]	[-0.917]	[0.389]	[1.272]	[-0.648]	[1.251]	[-2.218]	[-0.311]	[-1.369]	[−1.127]	[1.462]	[-0.154]
Panel C: RC90 copula												
0.022	0.094	0.899	3.077	0.700	0.044	0.131	-0.002	-0.117	0.389	-0.058	-0.005	0.320
(0.008)	(0.010)	(0.060)	(0.059)	(0.057)	(0.030)	(0.023)	(0.005)	(0.021)	(0.066)	(0.013)	(0.012)	(0.043)
[−1.355]	[-1.302]	[1.539]	[0.597]	[-0.117]	[-0.861]	[0.296]	[-0.217]	[-1.326]	[1.064]	[0.586]	[-1.130]	[0.777]
Panel D: RC270 copula												
0.021	0.093	0.901	3.125	0.709	0.039	0.129	-0.002	-0.099	0.343	-0.013	-0.018	0.326
(0.007)	(0.012)	(0.012)	(0.080)	(0.049)	(0.034)	(0.024)	(0.003)	(0.024)	(0.050)	(0.010)	(0.010)	(0.039)
[0.882]	[-1.401]	[0.669]	[0.031]	[-0.961]	[-0.744]	[1.266]	[0.088]	[0.176]	[-0.596]	[1.198]	[0.016]	[-0.035]

Notes: This table reports the posterior means of each parameter, and the associated NSEs are shown in parentheses. The numbers in square brackets are the values of the Geweke (1992) convergence test statistic.

Table 7. Estimation results for the UnGARCH model with CAC 40 returns

ω_0	ω_1	ω_2	δ_0	δ_1	δ_2	φ_0	φ_1	φ_2	φ_3	b_0	b_1	b_2
Panel A: Frank copula												
0.020	0.094	0.901	2.512	0.590	0.219	0.094	0.006	-0.176	0.296	-0.082	0.048	0.325
(0.006)	(0.008)	(0.015)	(0.086)	(0.045)	(0.044)	(0.018)	(0.006)	(0.019)	(0.038)	(0.021)	(0.022)	(0.034)
[0.458]	[-0.444]	[0.429]	[0.639]	[1.623]	[-0.756]	[0.725]	[0.519]	[-0.143]	[-1.238]	[0.992]	[-1.241]	[0.593]
Panel B: FGM copula												
0.020	0.093	0.902	2.783	0.591	0.147	0.096	0.005	-0.177	0.308	-0.039	0.021	0.337
(0.006)	(0.011)	(0.144)	(0.141)	(0.041)	(0.073)	(0.021)	(0.008)	(0.015)	(0.032)	(0.014)	(0.016)	(0.033)
[0.946]	[0.384]	[-0.677]	[0.550]	[1.766]	[-0.745]	[0.877]	[-1.116]	[-0.872]	[0.646]	[−0.674]	[1.714]	[-0.157]
Panel C: RC90 copula												
0.020	0.095	0.899	2.314	0.505	0.269	0.111	0.005	-0.188	0.316	-0.038	-0.009	0.294
(0.006)	(0.009)	(0.009)	(0.107)	(0.050)	(0.055)	(0.017)	(0.007)	(0.024)	(0.042)	(0.006)	(0.010)	(0.024)
[−0.831]	[0.618]	[-0.430]	[0.055]	[0.868]	[-0.073]	[0.008]	[-1.133]	[0.394]	[-0.453]	[0.028]	[-0.111]	[0.390]
Panel D: RC270 copula												
0.020	0.094	0.900	2.321	0.528	0.269	0.096	0.006	-0.174	0.285	-0.008	-0.013	0.259
(0.007)	(0.011)	(0.012)	(0.162)	(0.094)	(0.087)	(0.017)	(0.007)	(0.019)	(0.036)	(0.009)	(0.010)	(0.024)
[−0.122]	[0.646]	[-0.497]	[-0.063]	[-0.213]	[0.126]	[1.313]	[-0.243]	[-2.300]	[-0.184]	[0.991]	[-0.243]	[0.175]

Notes: This table reports the posterior means of each parameter, and the associated NSEs are shown in parentheses. The numbers in square brackets are the values of the Geweke (1992) convergence test statistic.

Table 8. Estimation results for the AG model

ω_0	ω_1	ω_2	κ	φ_0	φ_1	φ_2	φ_3	α	b_0	b_1	b_2
Panel A: Constant Frank copula: S&P 500 returns											
0.019	0.043	0.947	1.115	0.242	-0.025	-0.251	0.507	-0.279			
(0.023)	(0.035)	(0.040)	(0.039)	(0.032)	(0.131)	(0.042)	(0.107)	(0.038)			
[−0.151]	[-0.135]	[0.191]	[-1.068]	[0.573]	[-0.435]	[-1.191]	[-0.397]	[-0.830]			
Panel B: Time-varying Frank copula: S&P 500 returns											
0.019	0.045	0.945	1.114	0.235	0.021	-0.250	0.499		-0.274	0.210	0.376
(0.018)	(0.027)	(0.031)	(0.031)	(0.051)	(0.179)	(0.042)	(0.094)		(0.086)	(0.104)	(0.130)
[−0.229]	[-0.767]	[0.331]	[−0.083]	[-1.023]	[0.244]	[0.564]	[-0.024]		[-1.024]	[1.110]	[-0.872]
Panel C: Constant Frank copula: FTSE 100 returns											
0.020	0.049	0.940	1.169	0.093	-0.018	-0.095	0.503	-0.040			
(0.027)	(0.044)	(0.052)	(0.041)	(0.044)	(0.128)	(0.058)	(0.086)	(0.060)			
[0.139]	[0.082]	[-0.041]	[-0.883]	[-1.073]	[-0.700]	[0.993]	[0.370]	[0.699]			
Panel D: Time-varying Frank copula: FTSE 100 returns											
0.020	0.049	0.940	1.169	0.094	-0.023	-0.095	0.507		-0.068	0.101	0.323
(0.020)	(0.031)	(0.035)	(0.039)	(0.045)	(0.151)	(0.055)	(0.101)		(0.054)	(0.084)	(0.107)
[−1.597]	[-1.086]	[0.798]	[−0.469]	[-1.390]	[-0.599]	[0.254]	[-0.073]		[-0.249]	[0.835]	[0.765]
Panel E: Constant Frank copula: DAX returns											
0.019	0.037	0.951	1.115	0.149	0.008	-0.065	0.496	-0.194			
(0.025)	(0.035)	(0.043)	(0.053)	(0.046)	(0.159)	(0.061)	(0.102)	(0.050)			
[1.065]	[1.074]	[-1.062]	[0.741]	[0.293]	[-0.791]	[-0.324]	[0.347]	[0.740]			
Panel F: Time-varying Frank copula: DAX returns											
0.020	0.039	0.948	1.118	0.150	-0.046	-0.072	0.500		-0.135	-0.001	0.314
(0.023)	(0.031)	(0.038)	(0.055)	(0.030)	(0.197)	(0.056)	(0.094)		(0.073)	(0.080)	(0.122)
[0.888]	[0.912]	[-0.881]	[0.476]	[-0.398]	[-1.202]	[-0.742]	[-0.762]		[-0.908]	[0.800]	[-1.052]
Panel G: Constant Frank copula: CAC 40 returns											
0.019	0.041	0.949	1.151	0.112	-0.045	-0.158	0.502	0.036			
(0.017)	(0.025)	(0.031)	(0.053)	(0.041)	(0.109)	(0.049)	(0.079)	(0.052)			
[0.866]	[0.591]	[-0.608]	[0.335]	[-0.022]	[0.797]	[0.531]	[0.196]	[0.503]			
Panel H: Time-varying Frank copula: CAC 40 returns											
0.021	0.045	0.942	1.154	0.109	0.003	-0.154	0.488		0.033	-0.019	0.318
(0.016)	(0.023)	(0.032)	(0.048)	(0.021)	(0.159)	(0.032)	(0.086)		(0.058)	(0.058)	(0.110)
[0.201]	[0.135]	[0.017]	[−0.306]	[-0.229]	[1.156]	[0.324]	[-1.841]		[-0.349]	[0.739]	[0.942]

Notes: This table reports the posterior means of each parameter, and the associated NSEs are shown in parentheses. The numbers in square brackets are the values of the Geweke (1992) convergence test statistic.

Table 9. Moment specification tests: S&P 500 returns

	$E[z_t]=0$	$E[z_t z_{t-1}]=0$	$E[z_t z_{t-2}]=0$	$E[z_t z_{t-3}]=0$	$E[z_t z_{t-4}]=0$	$E[w_t w_{t-1}]=0$	$E[w_t w_{t-2}]=0$	$E[w_t w_{t-3}]=0$	$E[w_t w_{t-4}]=0$
BBHP	0.005	-0.066**	-0.022	-0.026	0.017	-0.406**	0.328	0.016	0.051
	(0.072)	(6.933)	(0.812)	(1.298)	(0.561)	(6.950)	(2.367)	(0.030)	(0.299)
LRS	0.004	-0.046**	-0.019	-0.020	0.011	-0.198**	0.140	0.004	0.026
	(0.044)	(8.813)	(1.045)	(1.371)	(0.411)	(20.400)	(2.349)	(0.006)	(0.244)
UnGARCH-Frank	-0.010	-0.043*	0.023	0.000	0.003	-0.405*	0.342	0.001	0.058
	(0.661)	(4.650)	(2.460)	(0.000)	(0.115)	(5.770)	(2.475)	(0.000)	(0.367)
UnGARCH-FGM	-0.010	-0.043*	0.023	0.001	0.003	-0.400*	0.348	0.026	0.059
	(0.616)	(4.620)	(2.304)	(0.012)	(0.127)	(6.030)	(2.294)	(0.073)	(0.364)
UnGARCH-RC90	-0.010	-0.043*	0.023	0.001	0.003	-0.403*	0.355	0.025	0.049
	(0.656)	(4.730)	(2.291)	(0.005)	(0.086)	(5.520)	(2.241)	(0.065)	(0.277)
UnGARCH-RC270	-0.009	-0.042*	0.021	0.002	0.003	-0.401*	0.306	0.033	0.044
	(0.495)	(4.340)	(2.950)	(0.044)	(0.085)	(5.750)	(2.322)	(0.121)	(0.237)
AG-Con-Frank	0.000	-0.032*	0.071**	0.039*	0.043**	0.198	1.632 **	0.828*	0.831**
	(0.999)	(4.474)	(14.83)	(6.143)	(8.211)	(0.265)	(7.605)	(5.697)	(9.912)
AG-Con-FGM	-0.001	-0.032	0.069**	0.038*	0.042**	0.179	1.595**	0.812*	0.814**
	(0.945)	(4.794)	(14.47)	(5.873)	(7.925)	(0.226)	(7.495)	(5.596)	(9.804)
AG-Con-RC90	-0.001	-0.026	0.076**	0.043**	0.048**	0.290	1.776**	0.899*	0.907**
	(0.969)	(2.911)	(16.48)	(7.363)	(9.783)	(0.510)	(8.060)	(6.142)	(10.62)
AG-Con-RC270	-0.001	-0.031*	0.071**	0.039*	0.044 **	0.203	1.636**	0.831*	0.834**
	(0.972)	(4.350)	(14.93)	(6.201)	(8.316)	(0.279)	(7.623)	(5.715)	(9.966)
AG-TV-Frank	-0.001	-0.034*	0.068**	0.037*	0.041**	0.159	1.564**	0.797*	0.797**
	(0.940)	(5.232)	(14.10)	(5.622)	(7.577)	(0.182)	(7.396)	(5.503)	(9.629)
AG-TV-FGM	0.000	-0.034*	0.068**	0.037*	0.041**	0.161	1.572**	0.801*	0.800**
	(0.980)	(5.223)	(14.12)	(5.651)	(7.588)	(0.184)	(7.411)	(5.516)	(9.626)
AG-TV-RC90	0.001	-0.039**	0.063**	0.034*	0.037*	0.086	1.469**	0.753*	0.743**
	(0.967)	(7.000)	(12.66)	(4.725)	(6.342)	(0.058)	(6.994)	(5.122)	(8.913)
AG-TV-RC270	-0.001	-0.029	0.073**	0.041**	0.045**	0.241	1.692**	0.858*	0.864**
	(0.944)	(3.660)	(15.61)	(6.690)	(8.965)	(0.375)	(7.811)	(5.898)	(10.28)

Notes: For the moment conditions listed in the column headings the table reports the corresponding sample averages and test statistics in parenthesis, which each follow a $\chi^2(1)$ distribution if the listed model is correctly specified. The superscripts *,** denote significance at the 5% and 1% levels, respectively.

Table 10. Moment specification tests: FTSE 100 returns

	$E[z_t]=0$	$E[z_t z_{t-1}]=0$	$E[z_t z_{t-2}]=0$	$E[z_t z_{t-3}]=0$	$E[z_t z_{t-4}]=0$	$E[w_t w_{t-1}]=0$	$E[w_t w_{t-2}]=0$	$E[w_t w_{t-3}]=0$	$E[w_t w_{t-4}]=0$
BBHP	-0.004	-0.039	-0.016	-0.046*	0.021	-0.088	0.059	0.028	0.056
	(0.036)	(3.138)	(0.562)	(4.922)	(1.061)	(0.953)	(0.936)	(0.201)	(0.439)
LRS	-0.003	-0.034*	-0.016	-0.037*	0.019	-0.039	0.043	0.037	0.065
	(0.027)	(4.044)	(0.877)	(4.489)	(1.112)	(0.675)	(1.332)	(0.706)	(0.8964)
UnGARCH-Frank	-0.001	-0.008	0.015	0.008	0.002	-0.083	0.069	0.038	0.055
	(0.014)	(0.772)	(3.538)	(0.901)	(0.031)	(0.815)	(1.173)	(0.335)	(0.416)
UnGARCH-FGM	-0.001	-0.007	0.013	0.006	0.002	-0.066	0.064	0.029	0.062
	(0.010)	(0.535)	(2.677)	(0.646)	(0.038)	(0.490)	(1.163)	(0.230)	(0.522)
UnGARCH-RC90	-0.002	-0.006	0.015	0.007	0.001	-0.076	0.058	0.030	0.059
	(0.038)	(0.477)	(3.331)	(0.714)	(0.020)	(0.669)	(0.867)	(0.219)	(0.482)
UnGARCH-RC270	-0.001	-0.008	0.014	0.007	0.001	-0.094	0.049	0.031	0.048
	(0.005)	(0.832)	(2.881)	(0.680)	(0.021)	(1.122)	(0.646)	(0.234)	(0.339)
AG-Con-Frank	0.002	0.007	0.045**	0.040 **	0.032*	0.385	0.702 **	0.790	0.605
	(0.878)	(0.278)	(11.70)	(7.983)	(5.570)	(3.646)	(11.51)	(7.144)	(6.447)
AG-Con-FGM	0.002	0.008	0.046 **	0.040**	0.033*	0.391	0.702**	0.792**	0.608**
	(0.901)	(0.344)	(11.97)	(8.205)	(5.770)	(3.823)	(11.76)	(7.297)	(6.646)
AG-Con-RC90	0.002	0.010	0.047 **	0.041**	0.034*	0.408*	0.708**	0.801**	0.624**
	(0.902)	(0.526)	(12.75)	(8.808)	(6.304)	(4.249)	(12.66)	(7.665)	(7.119)
AG-Con-RC270	0.002	0.004	0.044**	0.038**	0.030*	0.361	0.702 **	0.781**	0.594*
	(0.858)	(0.107)	(10.75)	(7.225)	(4.910)	(3.073)	(10.51)	(6.653)	(5.780)
AG-TV-Frank	0.002	0.007	0.045 **	0.039**	0.032*	0.384	0.701**	0.789**	0.604*
	(0.890)	(0.273)	(11.67)	(7.956)	(5.548)	(3.633)	(11.46)	(7.134)	(6.431)
AG-TV-FGM	0.002	0.008	0.046**	0.040**	0.033*	0.390	0.705**	0.793**	0.612*
	(0.895)	(0.324)	(12.03)	(8.205)	(5.754)	(3.765)	(11.95)	(7.243)	(6.584)
AG-TV-RC90	0.001	0.011	0.048**	0.042**	0.035*	0.417*	0.711**	0.804**	0.632**
	(0.916)	(0.644)	(13.12)	(9.120)	(6.592)	(4.512)	(13.06)	(7.903)	(7.410)
AG-TV-RC270	0.002	0.013	0.049 **	0.044**	0.037**	0.441*	0.726**	0.821**	0.662**
	(0.880)	(0.934)	(14.18)	(9.925)	(7.304)	(5.051)	(14.38)	(8.380)	(7.968)

Notes: For the moment conditions listed in the column headings the table reports the corresponding sample averages and test statistics in parenthesis, which each follow a $\chi^2(1)$ distribution if the listed model is correctly specified. The superscripts *,** denote significance at the 5% and 1% levels, respectively.

Table 11. Moment specification tests: DAX returns

	$E[z_t]=0$	$E[z_tz_{t-1}]=0$	$E[z_tz_{t-2}]=0$	$E[z_tz_{t-3}]=0$	$E[z_tz_{t-4}]=0$	$E[w_tw_{t-1}]=0$	$E[w_tw_{t-2}]=0$	$E[w_tw_{t-3}]=0$	$E[w_tw_{t-4}]=0$
BHHP	0.013	0.003	0.024	-0.022	0.018	-0.297**	0.195	0.128	0.020
	(0.473)	(0.022)	(1.214)	(1.061)	(0.736)	(11.99)	(2.491)	(1.229)	(0.037)
LRS	0.011	-0.002	0.019	-0.017	0.015	-0.134**	0.111	0.065	0.031
	(0.397)	(0.010)	(1.077)	(0.948)	(0.772)	(9.781)	(3.099)	(1.127)	(0.199)
UnGARCH-Frank	-0.008	-0.030	0.021*	0.011	-0.002	-0.309*	0.275	0.102	0.020
	(0.487)	(1.13)	(4.870)	(1.647)	(0.040)	(4.92)	(3.501)	(1.167)	(0.042)
UnGARCH-FGM	-0.009	-0.031	0.019*	0.011	-0.002	-0.308*	0.215	0.124	0.017
	(0.534)	(1.63)	(4.303)	(1.586)	(0.070)	(4.49)	(2.733)	(1.245)	(0.027)
UnGARCH-RC90	-0.009	-0.030	0.018*	0.010	-0.002	-0.300*	0.213	0.125	0.020
	(0.589)	(1.14)	(4.043)	(1.372)	(0.077)	(4.29)	(2.530)	(1.103)	(0.036)
UnGARCH-RC270	-0.008	-0.029	0.019*	0.011	-0.002	-0.293*	0.199	0.114	0.022
	(0.418)	(1.49)	(4.377)	(1.491)	(0.072)	(4.74)	(3.276)	(1.109)	(0.046)
AG-Con-Frank	0.001	-0.005	0.080**	0.064**	0.045**	0.566	1.612**	1.268*	0.821**
	(0.971)	(0.116)	(21.52)	(15.00)	(9.403)	(2.801)	(11.05)	(6.226)	(9.622)
AG-Con-FGM	0.000	-0.007	0.079**	0.062**	0.043**	0.548	1.570**	1.228*	0.793**
	(0.980)	(0.182)	(21.21)	(14.59)	(9.024)	(2.741)	(11.11)	(6.240)	(9.492)
AG-Con-RC90	0.000	-0.007	0.078**	0.062 **	0.043**	0.548	1.560**	1.214*	0.784**
	(0.990)	(0.214)	(20.88)	(14.28)	(8.697)	(2.771)	(11.06)	(6.166)	(9.425)
AG-Con-RC270	0.002	-0.009	0.076**	0.059**	0.040**	0.541	1.513**	1.157*	0.745**
	(0.905)	(0.365)	(20.05)	(13.39)	(7.901)	(2.693)	(11.08)	(6.130)	(9.163)
AG-TV-Frank	0.000	-0.007	0.078**	0.061**	0.042**	0.545	1.555**	1.208*	0.779**
	(0.974)	(0.228)	(20.81)	(14.20)	(8.632)	(2.748)	(11.05)	(6.157)	(9.371)
AG-TV-FGM	0.001	-0.008	0.077**	0.061**	0.042 **	0.543	1.543**	1.192*	0.769**
	(0.921)	(0.272)	(20.54)	(13.91)	(8.369)	(2.730)	(11.05)	(6.135)	(9.284)
AG-TV-RC90	0.000	-0.009	0.076 **	0.059**	0.041**	0.536	1.510**	1.159*	0.747**
	(0.986)	(0.343)	(20.27)	(13.58)	(8.096)	(2.682)	(11.13)	(6.184)	(9.221)
AG-TV-RC270	0.002	-0.009	0.077**	0.060**	0.041**	0.540	1.528 **	1.176*	0.758**
	(0.905)	(0.314)	(20.38)	(13.71)	(8.205)	(2.687)	(11.07)	(6.147)	(9.206)

Notes: For the moment conditions listed in the column headings the table reports the corresponding sample averages and test statistics in parenthesis, which each follow a $\chi^2(1)$ distribution if the listed model is correctly specified. The superscripts *,** denote significance at the 5% and 1% levels, respectively.

Table 12. Moment specification tests: CAC 40 returns

	$E[z_t]=0$	$E[z_tz_{t-1}]=0$	$E[z_tz_{t-2}]=0$	$E[z_tz_{t-3}]=0$	$E[z_tz_{t-4}]=0$	$E[w_tw_{t-1}]=0$	$E[w_tw_{t-2}]=0$	$E[w_tw_{t-3}]=0$	$E[w_tw_{t-4}]=0$
BHHP	-0.001	-0.020	-0.020	-0.044*	0.003	-0.215*	0.088	0.130	0.083
	(0.002)	(0.834)	(0.747)	(3.896)	(0.016)	(3.906)	(0.830)	(1.178)	(0.421)
LRS	-0.003	-0.018	-0.019	-0.034	0.004	-0.105*	0.051	0.080	0.069
	(0.028)	(1.182)	(1.141)	(3.619)	(0.044)	(5.021)	(1.193)	(1.693)	(0.669)
UnGARCH-Frank	0.000	-0.022	0.016	0.014	-0.001	-0.209	0.073	0.110	0.080
	(3.739)	(1.952)	(2.926)	(2.275)	(0.006)	(3.253)	(0.579)	(0.923)	(0.377)
UnGARCH-FGM	0.000	-0.023	0.017	0.015	-0.001	-0.233*	0.122	0.137	0.062
	(9.342)	(2.301)	(3.256)	(2.529)	(0.012)	(4.647)	(1.473)	(1.269)	(0.237)
UnGARCH-RC90	0.001	-0.024*	0.017	0.013	-0.001	-0.212	0.093	0.106	0.080
	(0.002)	(2.978)	(3.120)	(2.017)	(0.008)	(3.424)	(0.890)	(0.772)	(0.363)
UnGARCH-RC270	0.000	-0.024	0.017	0.015	-0.001	-0.220	0.091	0.143	0.085
	(0.001)	(4.176)	(3.239)	(2.322)	(0.005)	(3.818)	(0.826)	(1.112)	(0.411)
AG-Con-Frank	0.001	-0.014	0.042**	0.050**	0.029*	0.336	0.716*	1.015*	0.793*
	(0.941)	(1.042)	(9.541)	(10.78)	(4.019)	(1.403)	(6.363)	(5.656)	(5.058)
AG-Con-FGM	0.001	-0.016	0.041**	0.049**	0.028	0.307	0.695*	0.996*	0.764*
	(0.936)	(1.331)	(8.969)	(10.37)	(3.693)	(1.248)	(6.102)	(5.592)	(4.896)
AG-Con-RC90	0.002	-0.021	0.036**	0.045**	0.024	0.211	0.634*	0.937*	0.676*
	(0.902)	(2.601)	(7.274)	(9.101)	(2.735)	(0.741)	(5.424)	(5.513)	(4.402)
AG-Con-RC270	0.002	-0.021	0.036**	0.045**	0.024	0.211	0.633*	0.937*	0.675*
	(0.895)	(2.607)	(7.229)	(9.076)	(2.711)	(0.743)	(5.393)	(5.503)	(4.385)
AG-TV-Frank	0.002	-0.020	0.038**	0.046**	0.025	0.243	0.657*	0.959*	0.708*
	(0.879)	(2.121)	(7.835)	(9.522)	(3.049)	(0.908)	(5.655)	(5.534)	(4.581)
AG-TV-FGM	0.000	-0.019	0.038**	0.046**	0.026	0.255	0.654*	0.955*	0.708*
	(0.977)	(1.945)	(7.935)	(9.640)	(3.110)	(0.985)	(5.633)	(5.500)	(4.586)
AG-TV-RC90	0.002	-0.017	0.040**	0.048**	0.027	0.280	0.683*	0.984*	0.743*
	(0.886)	(1.639)	(8.548)	(10.04)	(3.450)	(1.098)	(5.962)	(5.583)	(4.794)
AG-TV-RC270	0.002	-0.018	0.039**	0.047**	0.026	0.265	0.672*	0.973*	0.728*
	(0.886)	(1.837)	(8.231)	(9.813)	(3.272)	(1.022)	(5.837)	(5.567)	(4.712)

Notes: For the moment conditions listed in the column headings the table reports the corresponding sample averages and test statistics in parenthesis, which each follow a $\chi^2(1)$ distribution if the listed model is correctly specified. The superscripts *,** denote significance at the 5% and 1% levels, respectively.

Table 13. Posterior model probabilities

	UnGARCH: S&P 500				UnGARCH: FTSE 100			
	Frank	FGM	RC90	RC270	Frank	FGM	RC90	RC270
UnGARCH-FGM	0.854				0.835			
UnGARCH-RC90	0.937	0.876			0.934	0.536		
UnGARCH-RC270	0.998	0.996	0.976		0.995	0.993	0.972	
BBHP	0.999	0.996	0.970	0.373	0.949	0.860	0.839	0.094
LRS	0.998	0.997	0.981	0.945	0.975	0.972	0.912	0.027
AG-Con-Frank	1.000	1.000	1.000	1.000	1.000	1.000	1.000	1.000
AG-Con-FGM	1.000	1.000	1.000	1.000	1.000	1.000	1.000	1.000
AG-Con-RC90	1.000	1.000	1.000	1.000	1.000	1.000	1.000	1.000
AG-Con-RC270	1.000	1.000	1.000	0.999	1.000	1.000	1.000	1.000
AG-TV-Frank	1.000	1.000	1.000	1.000	1.000	1.000	1.000	1.000
AG-TV-FGM	1.000	1.000	1.000	1.000	1.000	1.000	1.000	1.000
AG-TV-RC90	0.999	0.999	0.999	0.999	1.000	1.000	1.000	1.000
AG-TV-RC270	1.000	1.000	1.000	0.999	1.000	1.000	1.000	1.000
	UnGARCH: DAX				**UnGARCH: CAC 40**			
	Frank	FGM	RC90	RC270	Frank	FGM	RC90	RC270
UnGARCH-FGM	0.566				0.856			
UnGARCH-RC90	0.726	0.556			0.934	0.579		
UnGARCH-RC270	0.994	0.988	0.970		0.996	0.992	0.969	
BBHP	0.989	0.979	0.937	0.102	0.985	0.976	0.925	0.083
LRS	0.991	0.983	0.943	0.062	0.993	0.990	0.951	0.184
AG-Con-Frank	1.000	1.000	1.000	1.000	1.000	1.000	1.000	1.000
AG-Con-FGM	1.000	1.000	1.000	1.000	1.000	1.000	1.000	1.000
AG-Con-RC90	1.000	1.000	1.000	1.000	1.000	1.000	1.000	1.000
AG-Con-RC270	1.000	1.000	1.000	0.999	1.000	1.000	1.000	1.000
AG-TV-Frank	1.000	1.000	1.000	1.000	1.000	1.000	1.000	1.000
AG-TV-FGM	1.000	1.000	1.000	1.000	1.000	1.000	1.000	1.000
AG-TV-RC90	0.999	0.999	0.999	0.999	1.000	1.000	1.000	1.000
AG-TV-RC270	1.000	1.000	1.000	0.999	1.000	1.000	1.000	1.000

Notes: The entries correspond to the posterior probabilities of the models listed in the column headings versus each model listed on the rows, in turn.

Table 14. Out-of-sample forecasting results

	S&P 500		FTSE 100		DAX		CAC 40	
	RMSE	MAE	RMSE	MAE	RMSE	MAE	RMSE	MAE
UnGARCH-Frank	**0.981**	**0.997**	**0.994**	**0.998**	**1.004**	1.005	**0.992**	**1.000**
UnGARCH-FGM	0.996	1.001	0.995	**0.998**	1.005	1.005	0.994	1.001
UnGARCH-RC90	1.007	1.004	0.998	0.999	1.009	1.006	1.000	1.003
UnGARCH-RC270	1.019	1.011	1.006	1.004	1.008	**1.003**	1.008	1.002
AG-Con-Frank	0.999	1.001	1.015	1.005	1.012	1.005	0.997	1.001
AG-Con-FGM	1.041	1.009	1.019	1.003	1.012	1.004	0.999	1.001
AG-Con-RC90	1.020	1.008	1.008	1.002	1.005	1.004	1.021	1.008
AG-Con-RC270	1.027	1.004	0.998	0.999	**1.004**	**1.003**	1.036	1.011
AG-TV-Frank	1.034	1.007	0.996	0.999	1.009	1.004	0.995	1.003
AG-TV-FGM	1.011	1.004	1.018	1.012	1.010	**1.003**	0.995	1.001
AG-TV-RC90	1.037	1.005	1.005	1.003	**1.004**	**1.003**	0.998	1.002
AG-TV-RC270	1.053	1.027	1.009	1.006	1.013	1.008	1.008	1.005

Notes: The entries are ratios computed as the RMSE (MAE) for each model's forecast relative to the corresponding loss of the "no change" benchmark forecasts associated with a random walk model. A ratio less (greater) than 1 indicates that the model has a smaller (larger) loss than the benchmark. The smallest relative losses are shown in bold.

Table 15. Mincer-Zarnowitz regression results

	S&P 500			FTSE 100			DAX			CAC 40		
	$\hat{a}_0$	$\hat{a}_1$	p-value	$\hat{a}_0$	$\hat{a}_1$	p-value	$\hat{a}_0$	$\hat{a}_1$	p-value	$\hat{a}_0$	$\hat{a}_1$	p-value
UnGARCH-Frank	-0.013	0.622	0.539	-0.059	1.236	0.422	-0.015	0.221	0.078	-0.068	0.924	0.231
	(0.040)	(0.370)		(0.046)	(0.506)		(0.041)	(0.247)		(0.048)	(0.593)	
UnGARCH-FGM	-0.010	0.531	0.520	-0.062	1.246	0.367	-0.015	0.225	0.147	-0.066	0.867	0.223
	(0.040)	(0.441)		(0.044)	(0.408)		(0.041)	(0.246)		(0.047)	(0.556)	
UnGARCH-RC90	0.002	0.234	0.198	0.003	0.930	0.991	-0.006	0.126	0.092	-0.029	0.067	0.495
	(0.037)	(0.436)		(0.034)	(0.693)		(0.042)	(0.292)		(0.042)	(0.497)	
UnGARCH-RC270	-0.010	-0.237	**0.022**	-0.030	-0.896	**0.050**	-0.005	0.038	0.061	-0.047	-0.503	**0.021**
	(0.038)	(0.452)		(0.039)	(0.783)		(0.039)	(0.209)		(0.042)	(0.545)	
AG-Con-Frank	-0.096	1.265	0.145	-0.003	-0.151	**0.001**	-0.019	0.116	**0.002**	-0.107	1.018	0.061
	(0.051)	(0.513)		(0.035)	(0.317)		(0.049)	(0.321)		(0.053)	(0.376)	
AG-Con-FGM	0.007	-0.261	**0.006**	0.005	-0.368	**0.014**	-0.007	-0.003	**0.012**	-0.076	0.705	0.092
	(0.038)	(0.427)		(0.038)	(0.492)		(0.045)	(0.384)		(0.055)	(0.579)	
AG-Con-RC90	-0.038	1.693	0.330	-0.010	-0.014	0.328	-0.011	0.096	**0.036**	-0.043	-0.124	**0.016**
	(0.043)	(0.510)		(0.039)	(0.707)		(0.049)	(0.419)		(0.040)	(0.459)	
AG-Con-RC270	-0.005	-0.120	**0.009**	-0.025	0.699	0.477	-0.026	0.303	**0.034**	-0.048	-0.598	**0.000**
	(0.037)	(0.365)		(0.037)	(0.379)		(0.049)	(0.345)		(0.042)	(0.177)	
AG-TV-Frank	0.004	-0.156	**0.003**	-0.071	1.012	0.187	-0.033	0.275	**0.000**	-0.103	1.099	0.105
	(0.040)	(0.375)		(0.047)	(0.353)		(0.053)	(0.221)		(0.057)	(0.471)	
AG-TV-FGM	-0.022	0.227	**0.013**	-0.032	0.240	**0.000**	-0.033	0.225	**0.000**	-0.054	0.301	**0.010**
	(0.044)	(0.350)		(0.042)	(0.174)		(0.045)	(0.176)		(0.043)	(0.306)	
AG-TV-RC90	0.000	-0.191	**0.005**	-0.024	0.357	**0.008**	-0.035	0.385	**0.000**	-0.051	0.847	0.342
	(0.037)	(0.372)		(0.041)	(0.265)		(0.049)	(0.170)		(0.045)	(0.360)	
AG-TV-RC270	-0.066	-0.704	**0.000**	-0.015	-0.111	0.099	-0.020	-0.140	**0.000**	-0.040	0.079	0.101
	(0.038)	(0.293)		(0.041)	(0.554)		(0.043)	(0.279)		(0.045)	(0.431)	

Notes: This table reports estimates of the intercept (a_0) and slope (a_1) parameters in Mincer-Zarnowitz regressions of realized returns on the mean returns predicted from the different models. Newey-West HAC standard errors are shown in parentheses and the reported p-values correspond to Wald tests of the joint hypothesis $a_0 = 0$, $a_1 = 1$. The p-values $\leq 5\%$ are shown in bold.

Table 16. VaR violation ratios

	$p = 0.01$				$p = 0.05$			
	S&P 500	FTSE 100	DAX	CAC 40	S&P 500	FTSE 100	DAX	CAC 40
BBHP	0.38	0.37	0.44	0.22	**0.86**	**0.90**	**0.86**	**0.84**
LRS	1.50	0.75	0.67	0.66	1.88	1.89	1.79	1.95
UnGARCH-Frank	1.88	1.72	1.33	1.77	1.41	1.47	1.43	1.67
UnGARCH-FGM	1.73	1.87	1.18	1.55	1.41	1.53	1.42	1.62
UnGARCH-RC90	**1.50**	**1.05**	**1.03**	**1.03**	1.22	1.36	1.24	1.42
UnGARCH-RC270	1.95	1.65	1.26	1.25	1.37	1.38	1.32	1.52
AG-Con-Frank	2.33	1.20	2.00	1.33	1.53	1.53	1.51	1.56
AG-Con-FGM	2.10	1.27	1.92	1.25	1.50	1.54	1.46	1.58
AG-Con-RC90	1.88	1.35	1.55	1.18	1.40	1.39	1.29	1.45
AG-Con-RC270	1.88	1.20	1.55	1.18	1.38	1.42	1.40	1.42
AG-TV-Frank	2.10	1.27	1.70	1.18	1.55	1.53	1.55	1.50
AG-TV-FGM	2.70	3.60	2.29	2.51	1.70	1.89	1.60	1.65
AG-TV-RC90	1.73	1.57	1.55	1.18	1.50	1.42	1.51	1.45
AG-TV-RC270	1.95	1.22	1.70	0.86	1.50	1.50	1.27	1.37

Notes: This table reports the ratios $\hat{p}/p$ with bold entries indicating the model whose ratio is closest to one.

Table 17. Counts of VaR test rejections across the 4 markets

	$p = 0.01$			$p = 0.05$		
	UC	CC	DQ	UC	CC	DQ
BBHP	4	3	**1**	1	**1**	**0**
LRS	1	1	**1**	4	4	4
UnGARCH-Frank	3	3	3	3	2	3
UnGARCH-FGM	2	2	2	3	2	3
UnGARCH-RC90	**0**	**0**	**1**	**0**	**1**	1
UnGARCH-RC270	2	1	2	3	3	3
AG-Con-Frank	2	2	2	4	3	4
AG-Con-FGM	2	2	2	4	4	4
AG-Con-RC90	1	1	**1**	4	3	4
AG-Con-RC270	1	1	**1**	4	4	4
AG-TV-Frank	2	2	2	4	3	4
AG-TV-FGM	4	4	4	4	4	4
AG-TV-RC90	1	1	**1**	4	3	4
AG-TV-RC270	2	2	2	4	4	4

Notes: Significance is counted at the 5% level and bold entries indicate the model with the lowest number of rejections for each test.

Table 18. Penalty structure

Zone	Number of violations	k
Green	0–4	0
Yellow	5	0.40
	6	0.50
	7	0.65
	8	0.75
	9	0.85
Red	10+	1

Notes: The number of VaR violations is calculated over the last 250 trading days.

Table 19. Regulatory backtesting results

	S&P 500					FTSE 100				
	Capital charge	Penalty	Green	Yellow	Red	Capital charge	Penalty	Green	Yellow	Red
BBHP	15.03	0.00	1.00	0.00	0.00	13.73	0.00	1.00	0.00	0.00
LRS	13.01	0.18	0.66	0.33	0.01	12.03	0.04	0.91	0.09	0.00
UnGARCH-Frank	12.52	0.34	0.28	0.72	0.00	10.95	0.17	0.69	0.31	0.00
UnGARCH-FGM	12.33	0.27	0.51	0.49	0.00	11.08	0.22	0.58	0.42	0.00
UnGARCH-RC90	12.57	0.17	0.60	0.40	0.00	11.43	0.17	0.71	0.29	0.00
UnGARCH-RC270	12.41	0.34	0.28	0.72	0.00	11.18	0.18	0.65	0.35	0.00
AG-Con-Frank	13.22	0.41	0.38	0.53	0.09	11.24	0.16	0.72	0.28	0.00
AG-Con-FGM	13.15	0.36	0.42	0.51	0.08	11.37	0.08	0.83	0.17	0.00
AG-Con-RC90	13.61	0.28	0.54	0.42	0.04	11.26	0.09	0.83	0.17	0.00
AG-Con-RC270	13.71	0.32	0.43	0.53	0.04	11.21	0.08	0.83	0.17	0.00
AG-TV-Frank	13.01	0.37	0.38	0.58	0.04	11.18	0.09	0.83	0.17	0.00
AG-TV-FGM	13.30	0.53	0.33	0.38	0.29	11.46	0.23	0.71	0.11	0.18
AG-TV-RC90	13.25	0.27	0.54	0.45	0.02	11.18	0.10	0.77	0.23	0.00
AG-TV-RC270	13.15	0.33	0.42	0.56	0.03	11.07	0.08	0.83	0.17	0.00
	DAX					CAC 40				
	Capital charge	Penalty	Green	Yellow	Red	Capital charge	Penalty	Green	Yellow	Red
BBHP	16.33	0.00	1.00	0.00	0.00	16.90	0.00	1.00	0.00	0.00
LRS	13.61	0.00	1.00	0.00	0.00	13.72	0.00	1.00	0.00	0.00
UnGARCH-Frank	12.14	0.05	0.87	0.13	0.00	13.36	0.25	0.44	0.56	0.00
UnGARCH-FGM	11.97	0.03	0.93	0.07	0.00	12.92	0.15	0.67	0.33	0.00
UnGARCH-RC90	12.43	0.00	1.00	0.00	0.00	12.94	0.01	0.98	0.02	0.00
UnGARCH-RC270	12.48	0.10	0.79	0.21	0.00	12.45	0.01	0.98	0.02	0.00
AG-Con-Frank	13.68	0.38	0.47	0.31	0.22	13.41	0.19	0.59	0.41	0.00
AG-Con-FGM	13.68	0.34	0.55	0.26	0.19	13.41	0.19	0.56	0.44	0.00
AG-Con-RC90	13.94	0.27	0.59	0.34	0.06	13.68	0.17	0.61	0.39	0.00
AG-Con-RC270	13.85	0.27	0.59	0.34	0.06	13.56	0.13	0.72	0.28	0.00
AG-TV-Frank	13.46	0.31	0.55	0.33	0.11	13.28	0.16	0.61	0.39	0.00
AG-TV-FGM	13.75	0.46	0.40	0.40	0.20	14.59	0.51	0.24	0.54	0.22
AG-TV-RC90	13.45	0.24	0.69	0.22	0.10	13.30	0.08	0.82	0.18	0.00
AG-TV-RC270	13.70	0.28	0.66	0.14	0.20	13.00	0.03	0.94	0.06	0.00

Notes: This table reports the average capital charge and penalty, as well as the proportion of time spent in each penalty zone (green, yellow, red).

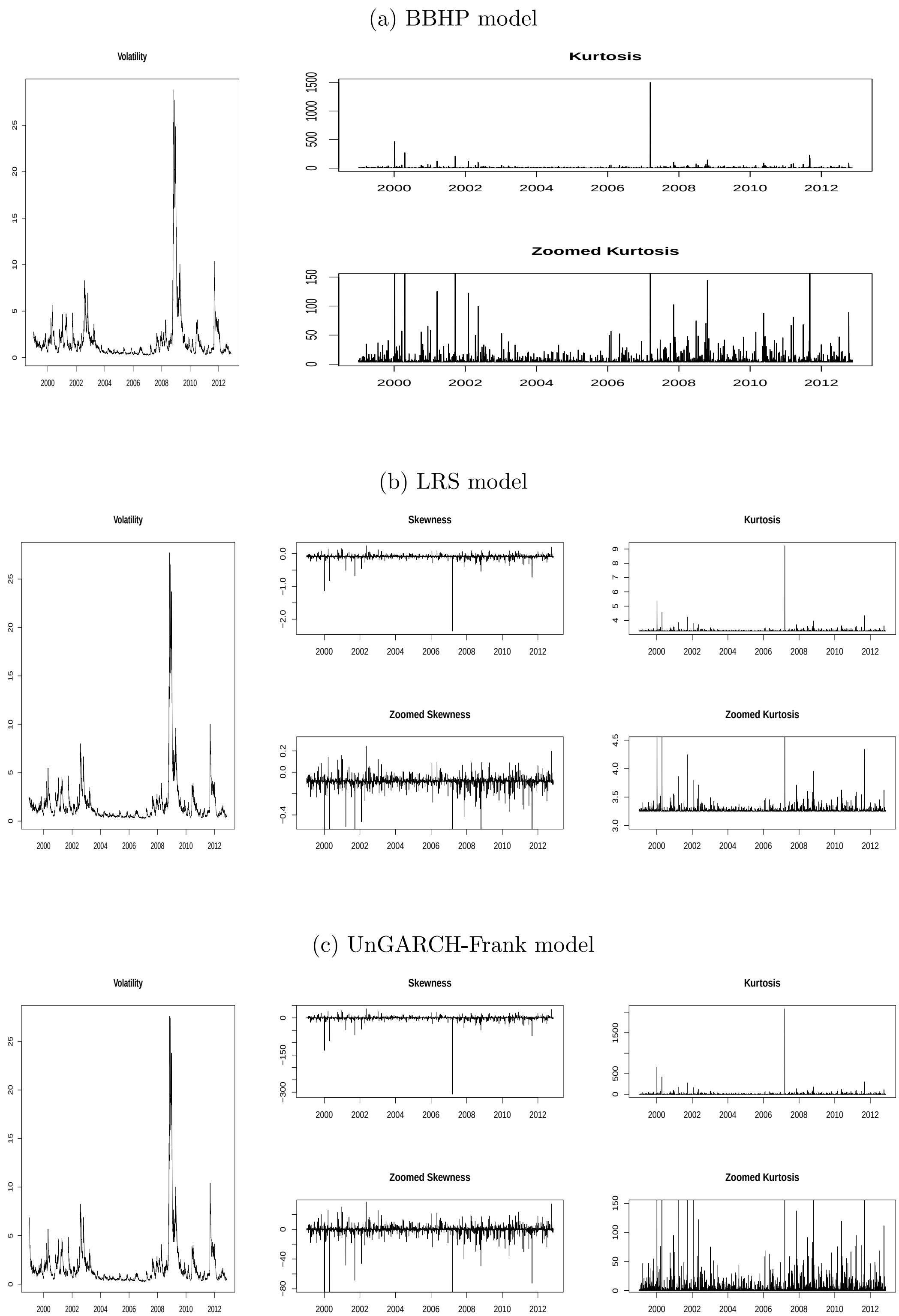

Figure 1. Model-implied conditional moments: S&P 500 returns

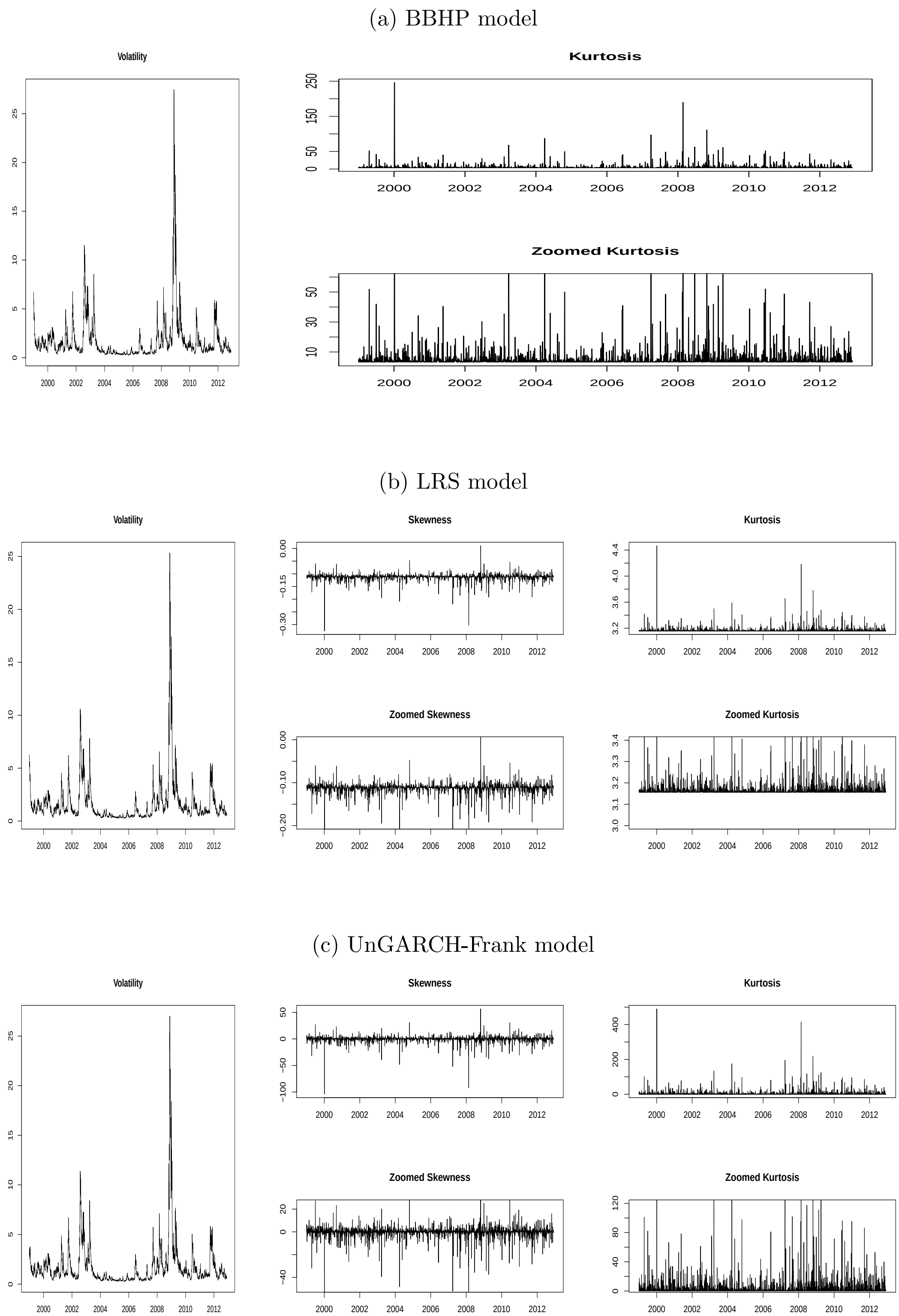

Figure 2. Model-implied conditional moments: FTSE 100 returns

(a) BBHP model

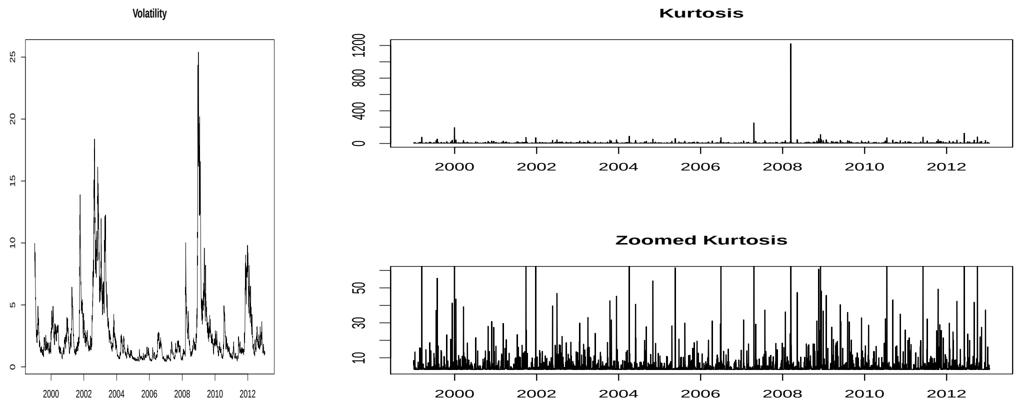

(b) LRS model

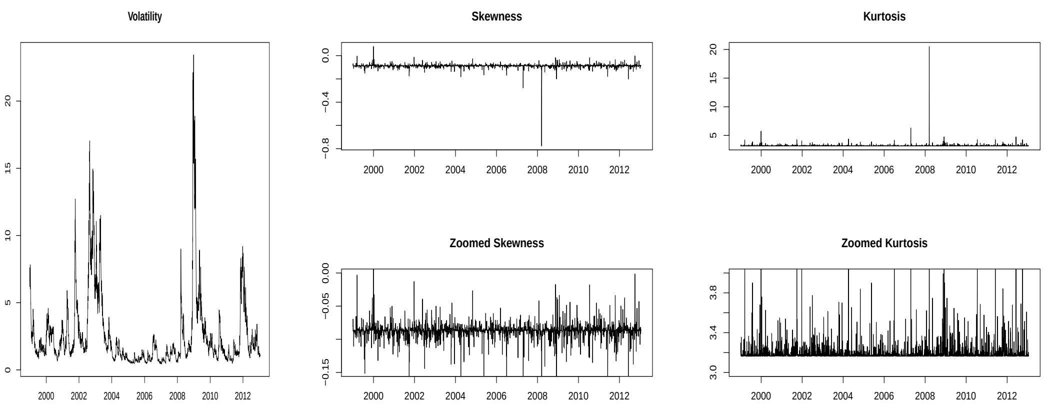

(c) UnGARCH-Frank model

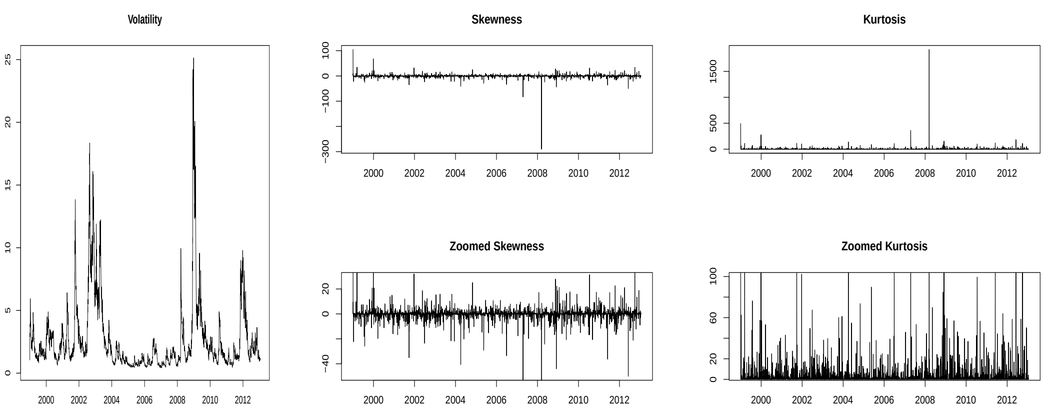

Figure 3. Model-implied conditional moments: DAX returns

(a) BBHP model

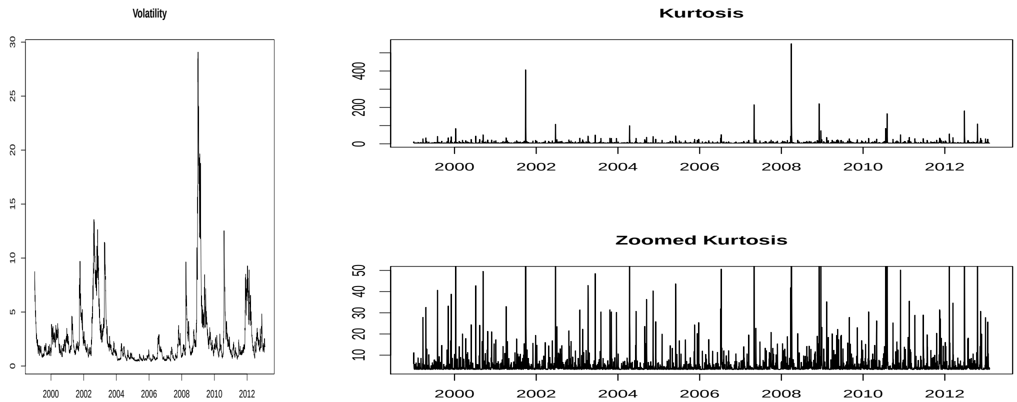

(b) LRS model

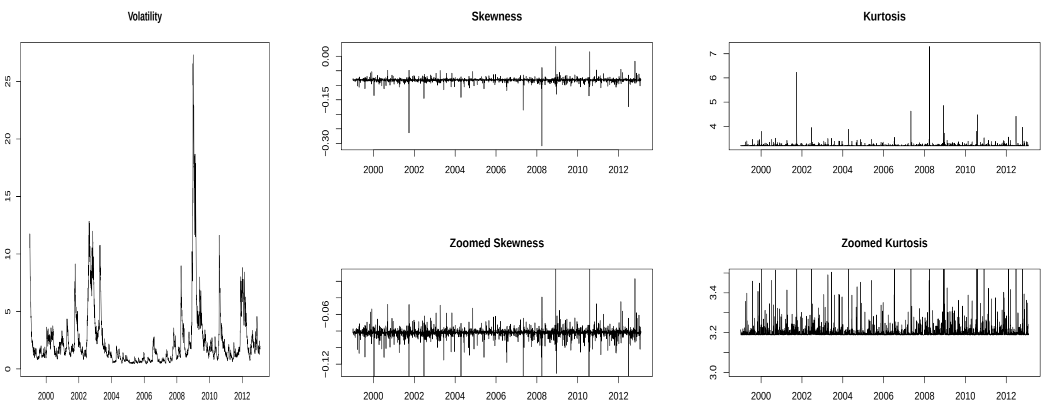

(c) UnGARCH-Frank model

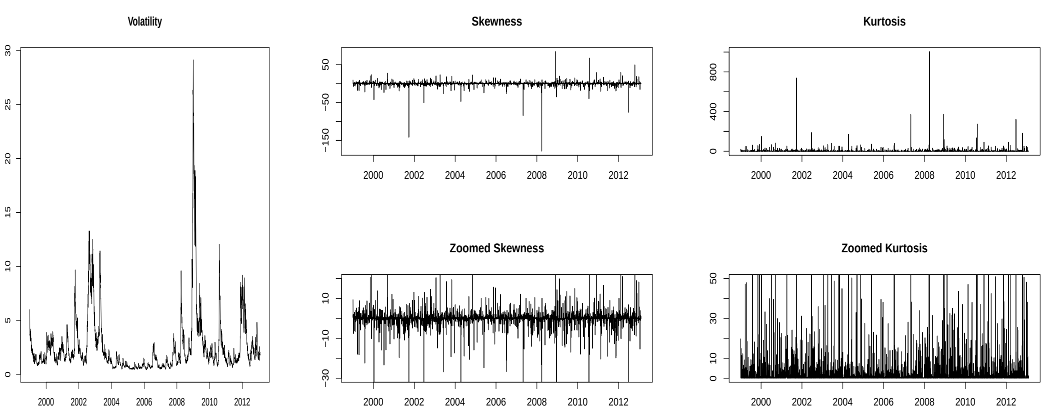

Figure 4. Model-implied conditional moments: CAC 40 returns

(a) AG-Con-Frank model

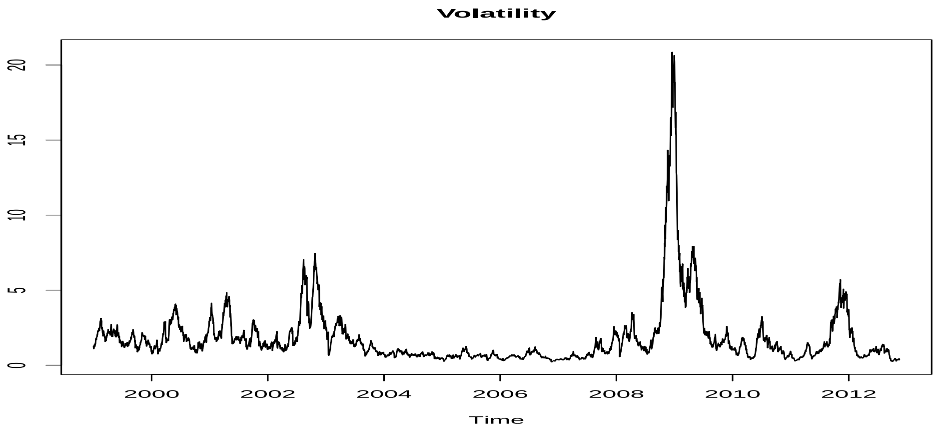

(b) AG-TV-Frank model

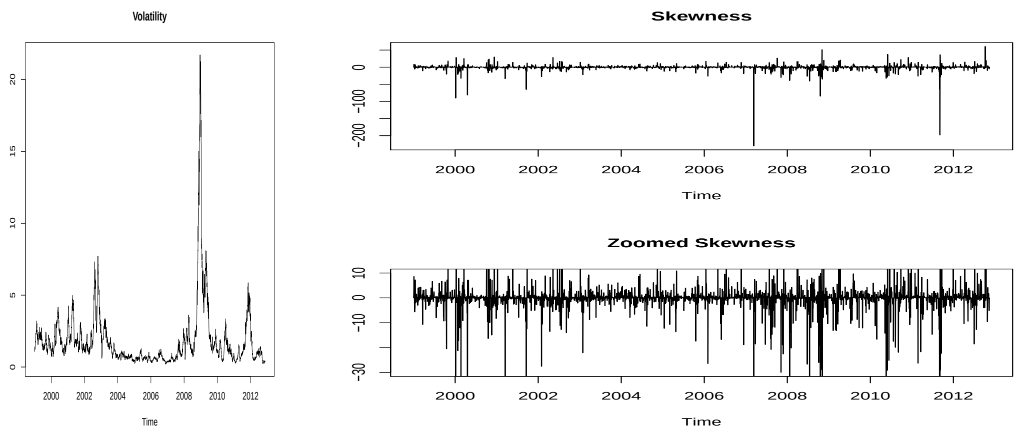

Figure 5. AG model-implied conditional moments: S&P 500 returns

(a) AG-Con-Frank model

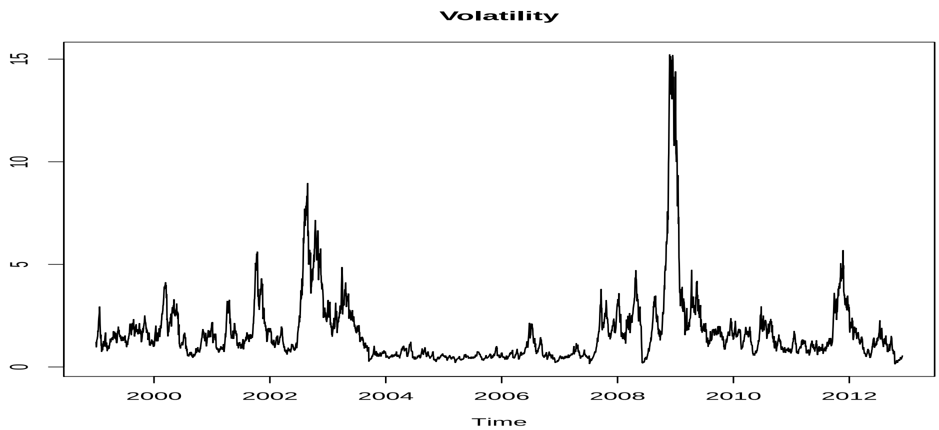

(b) AG-TV-Frank model

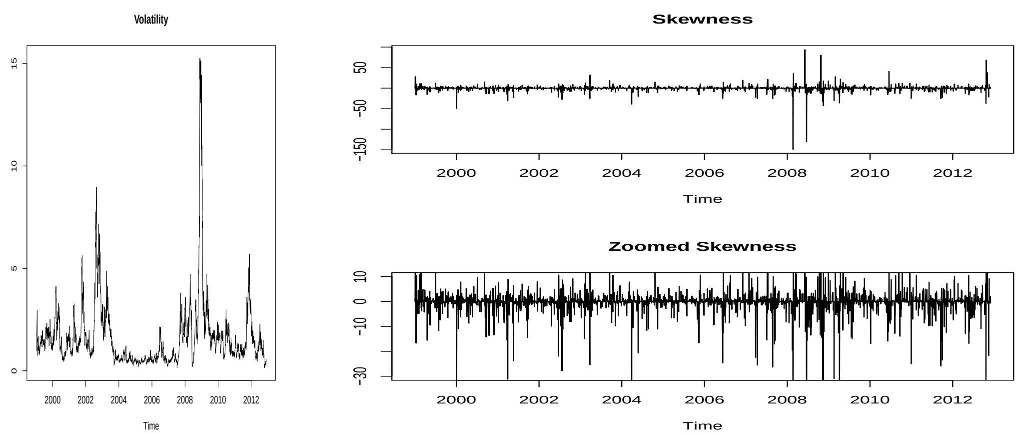

Figure 6. AG model-implied conditional moments: FTSE 100 returns

(a) AG-Con-Frank model

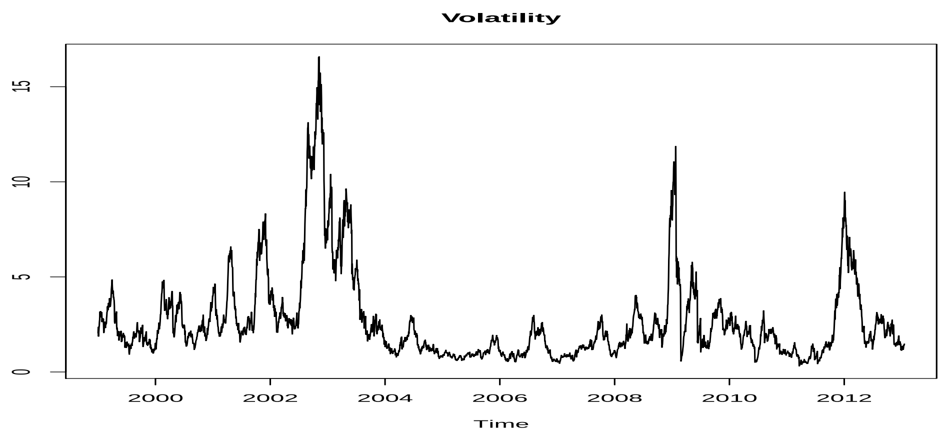

(b) AG-TV-Frank model

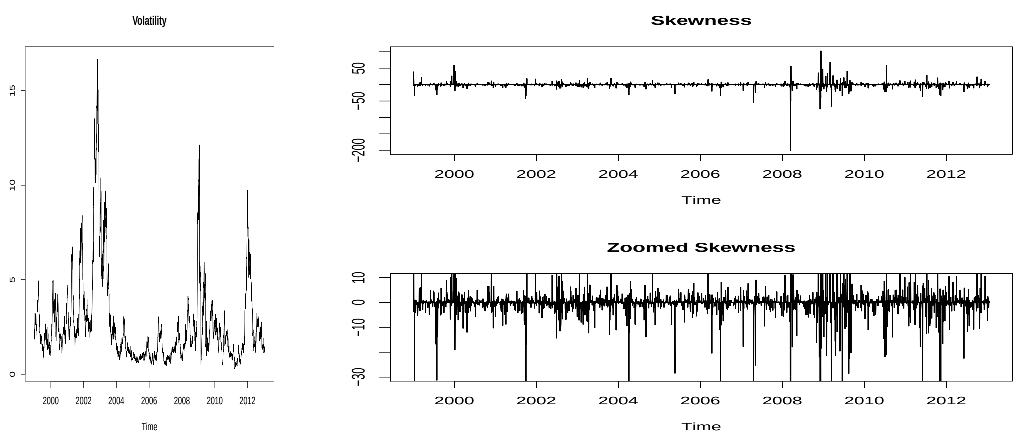

Figure 7. AG model-implied conditional moments: DAX returns

(a) AG-Con-Frank model

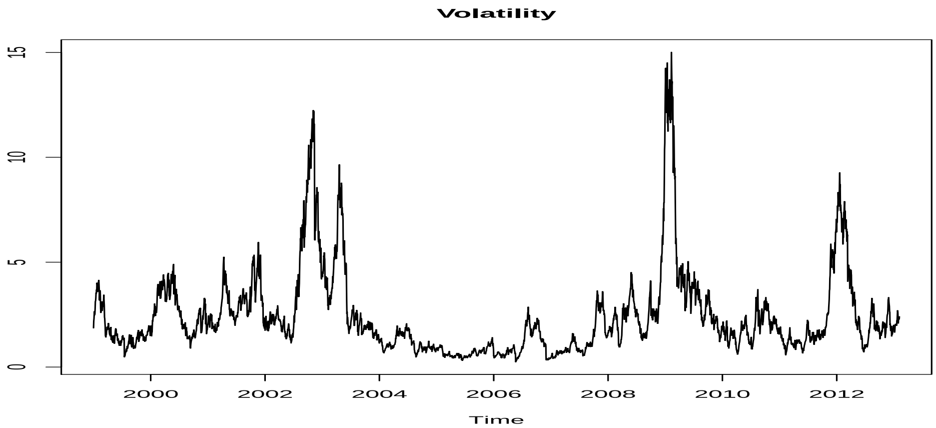

(b) AG-TV-Frank model

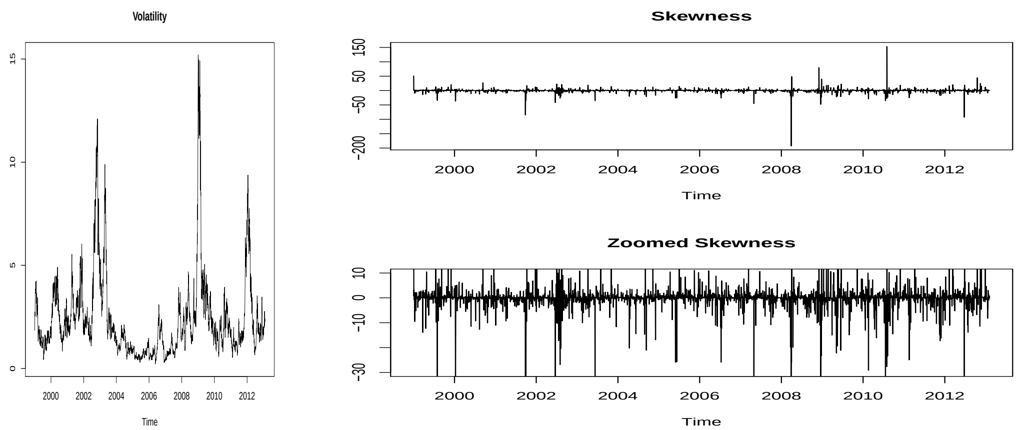

Figure 8. AG model-implied conditional moments: CAC 40 returns

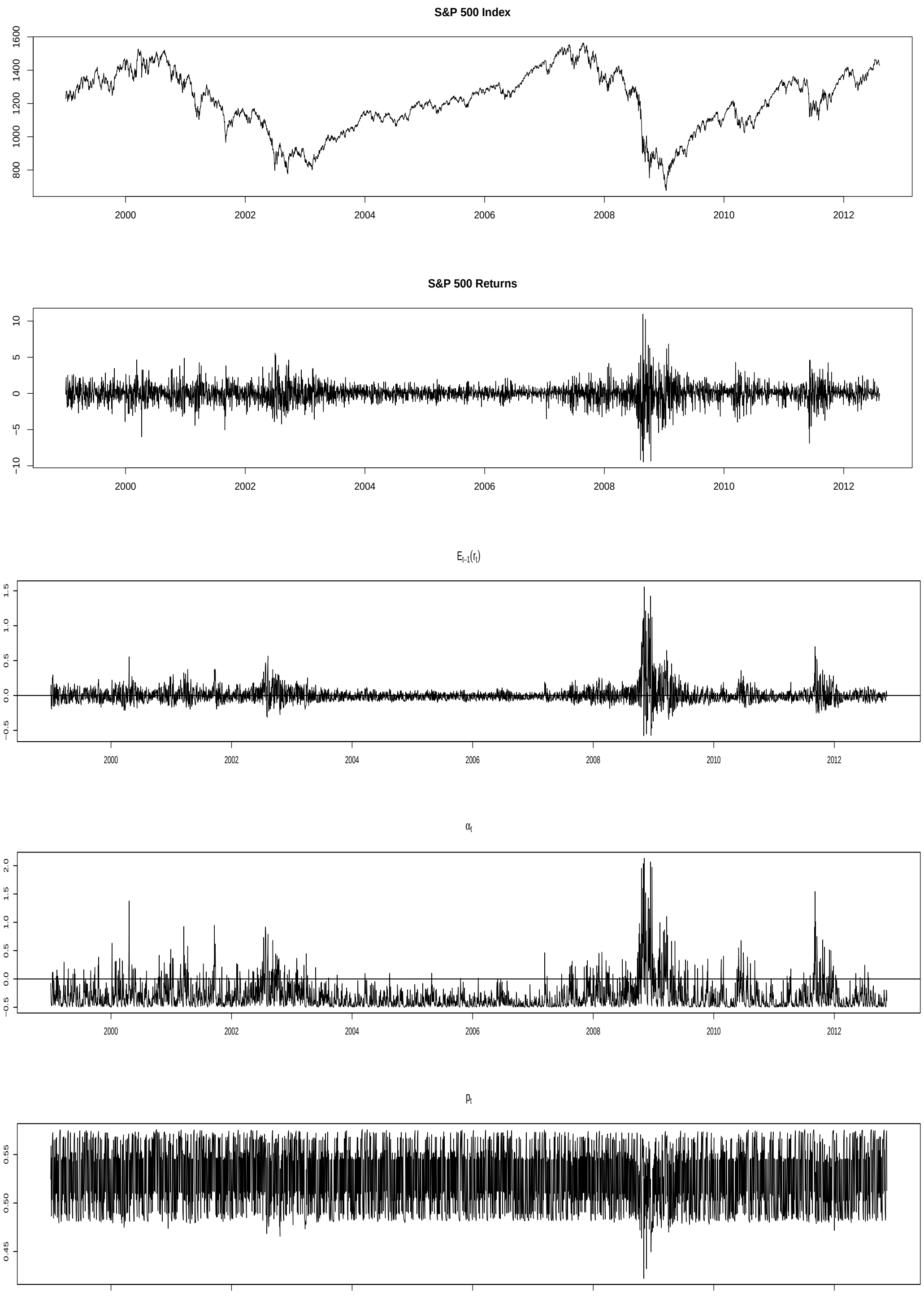

Figure 9. Time series of $E_{t-1}(R_t)$, α_t, and p_t: S&P 500 returns

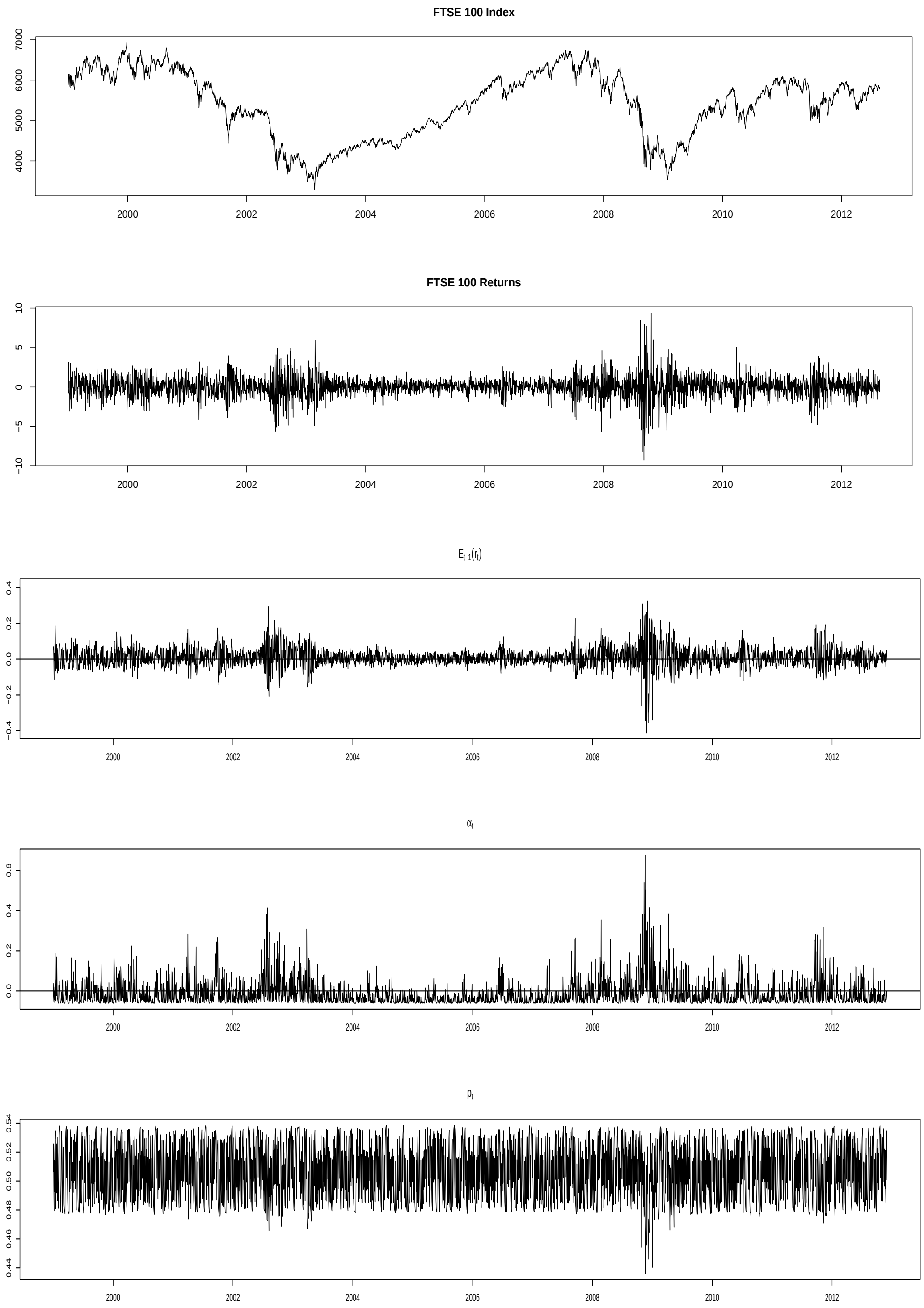

Figure 10. Time series of $E_{t-1}(R_t)$, α_t, and p_t: FTSE 100 returns

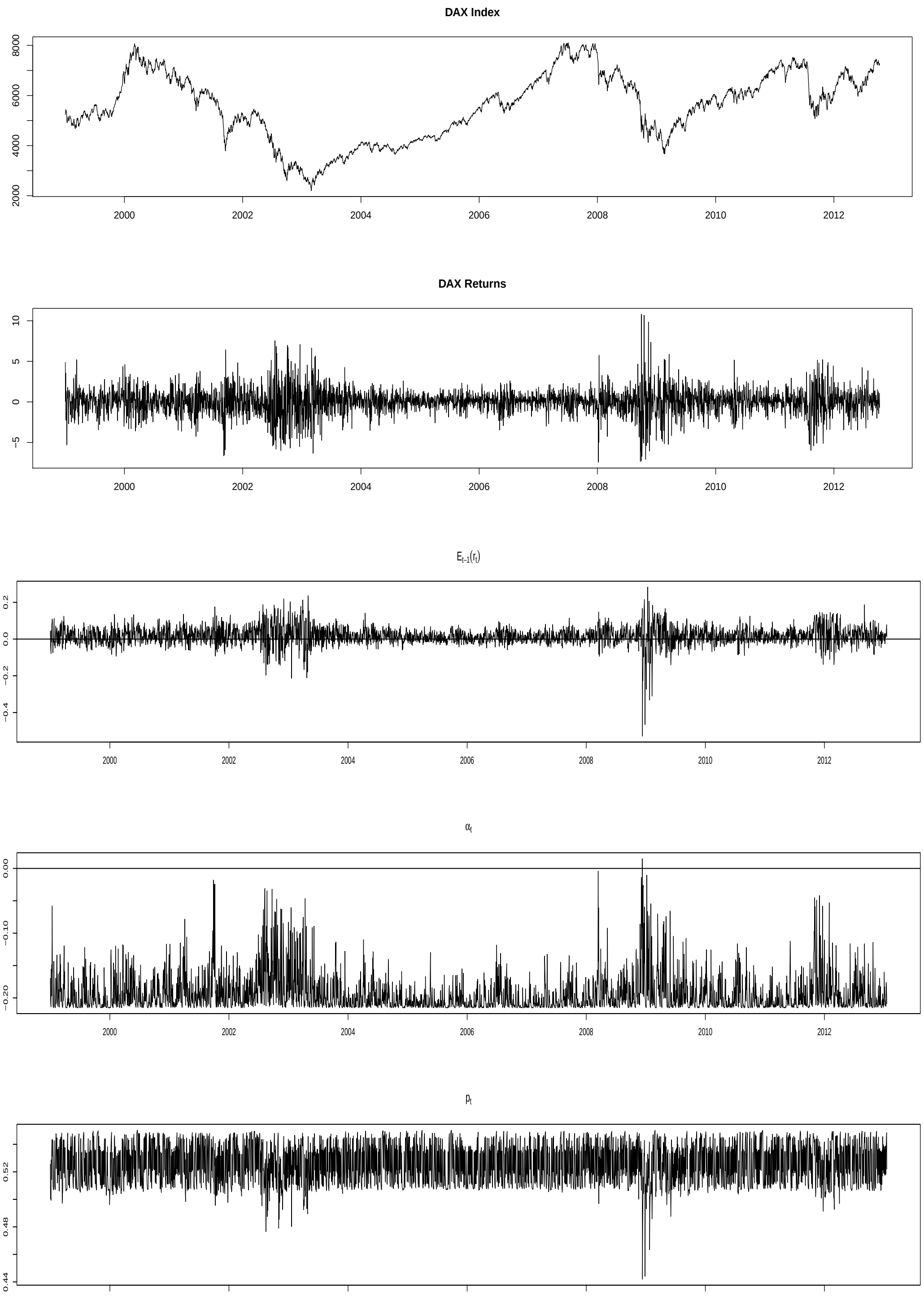

Figure 11. Time series of $E_{t-1}(R_t)$, α_t, and p_t: DAX returns

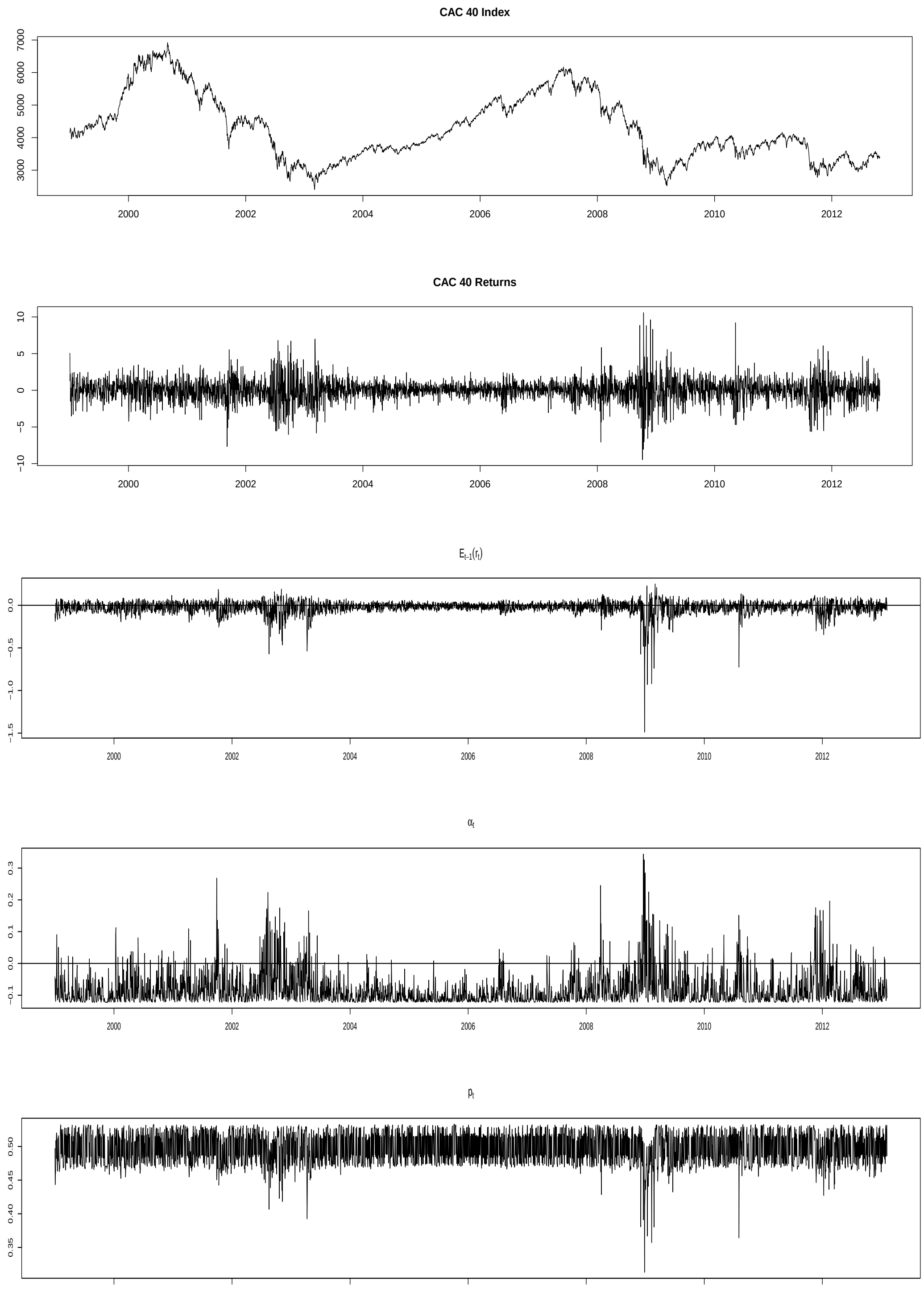

Figure 12. Time series of $E_{t-1}(R_t)$, α_t, and p_t: CAC 40 returns